

Collaboration between Trinuclear Aluminum Complexes Bearing Bipyrazoles in the Ring-Opening Polymerization of ϵ -Caprolactone

Someswara Rao Kosuru,[○] Feng-Jie Lai,[○] Yu-Lun Chang, Chen-Yu Li, Yi-Chun Lai, Shangwu Ding, Kuo-Hui Wu,^{*} Hsuan-Ying Chen,^{*} and Yung-Han Lo

Cite This: *Inorg. Chem.* 2021, 60, 10535–10549

Read Online

ACCESS |

Metrics & More

Article Recommendations

Supporting Information

ABSTRACT: Trinuclear aluminum complexes bearing bipyrazoles were synthesized, and their catalytic activity for ϵ -caprolactone (CL) polymerization was investigated. $D^{Bu}_2Al_3Me_5$ exhibited higher catalytic activity than did the dinuclear aluminum complex $L^{Bu}_2Al_2Me_4$ (16 times as high for CL polymerization; [CL]:[$D^{Bu}_2Al_3Me_5$]:[BnOH] = 100:0.5:5, [$D^{Bu}_2Al_3Me_5$] = 10 mM, conversion 93% after 18 min at room temperature). Density functional theory calculations revealed a polymerization mechanism in which CL first approached the central Al atom and then moved to an external Al. The coordinated CL ring was opened because the repulsion of two *tert*-butyl groups on the ligands pushed an alkoxide initiator on an external Al to initiate CL. In these trinuclear Al catalysts, the central Al plays a role in monomer capture and then collaborates with the external Al to activate CL, accelerating polymerization.



INTRODUCTION

The influence of petrochemical plastics on modern society is remarkable. However, environmental pollution caused by discarded plastic waste must be managed^{1–4} because discarded plastics do not quickly decompose naturally. To accelerate the environmental degradation of polymers and further the goal of a sustainable society, biodegradable poly- ϵ -caprolactone (PCL)⁵ has been developed. PCL-based biomaterials are used in various fields^{6–16} because of their biocompatibility^{5,17} and permeability.¹⁸ The primary method for manufacturing PCL is the Lewis acidic catalyzed ring-opening polymerization (ROP) of ϵ -caprolactone (CL).^{19–28}

Al catalysts are frequently used for ROP because they are strong Lewis acids, are easy to synthesize, and have inexpensive precursors. Ligands are essential for catalyst design because they can influence the catalytic activity through electronic,^{29–32} steric,^{31,33,34} chelating,^{31,35–37} and dinuclear cooperation effects^{29,38–40} and reduce transesterification.^{41,42} Recently, Al complexes^{43–49} bearing pyrazolyl-containing ligands and their application in ROP have been reported; these complexes exhibit moderate catalytic activity for cyclic ester polymerization. Importantly, dinuclear Al complexes²⁹ bearing pyrazolide derivatives (Figure 1a) with high catalytic activities for CL ROP have been reported. Such activities have been ascribed to electronic and dinuclear cooperation effects. To further investigate the catalytic activity in this class of molecules, a series of bipyrazoles and associated trinuclear Al complexes (Figure 1b and Scheme 1) were synthesized, and

the catalytic activities of trinuclear Al complexes for CL polymerization were investigated.

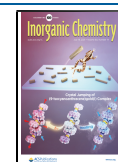
RESULTS AND DISCUSSION

Synthesis and Characterization of Al Complexes.

Alkane- and arene-1,3,4,6-tetraketones were prepared using methods based on those described in the literature.^{50,51} A series of bipyrazoles was synthesized through the condensation reaction of hydrazine hydrate and an alkane- or arene-1,3,4,6-tetraketone (2:1 ratio). $D^{Bu}_2Al_3Me_5$, $D^{Ad}_2Al_3Me_5$, $D^{Pr}_2Al_3Me_5$, $D^{Tol}_2Al_3Me_5$, and $D^{Ph}_2Al_3Me_5$ were synthesized through the reaction of bipyrazole ligands and $AlMe_3$ (2:3 ratio). The products of these ligands, including D^{Cl-H} and D^{Br-H} , are insoluble in organic solvents, including dimethyl sulfoxide and dimethylformamide. The formation of the bipyrazole ligands and associated Al complexes was verified through nuclear magnetic resonance (NMR) spectroscopy. The ¹H NMR peak of the four methine groups of two D^{Bu-H} s (at 6.30 ppm in $CDCl_3$) shifted to 6.49 ppm after reaction with $AlMe_3$, and the presence of five methyl groups on Al atoms was observed (at -0.18 , -0.48 , and -0.99 ppm in $CDCl_3$; integration ratio = 2:2:1 (Figure S6)). The ligands, including D^{Bu-H} , D^{Ad-H} , D^{Pr-H} ,

Received: April 19, 2021

Published: July 7, 2021



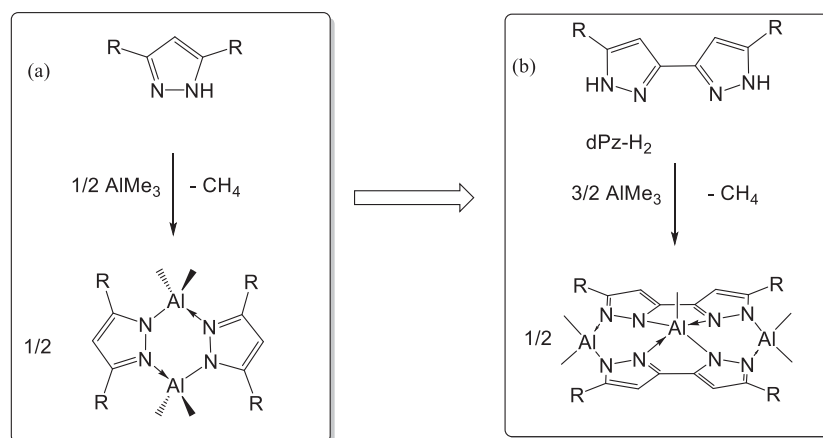
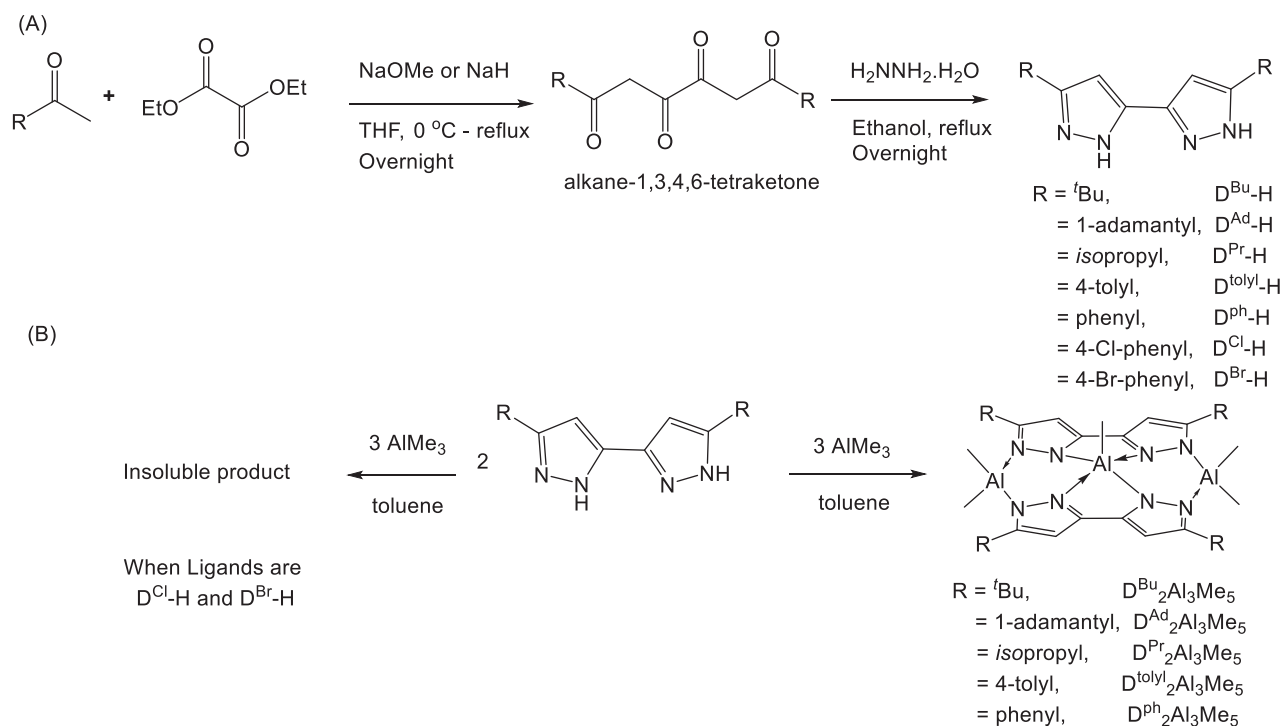


Figure 1. Dinuclear and trinuclear Al complexes bearing pyrazolyl-containing ligands.

Scheme 1. Synthesis of (A) Bipyrazole Ligands and (B) Associated Al Complexes



H, $\text{D}^{\text{tolyl-H}}$, $\text{D}^{\text{ph-H}}$, $\text{D}^{\text{Cl-H}}$, and $\text{D}^{\text{Br-H}}$, are not insoluble in CDCl_3 ; however, $\text{D}^{\text{Ad}_2\text{Al}_3\text{Me}_5}$, $\text{D}^{\text{Pr}_2\text{Al}_3\text{Me}_5}$, $\text{D}^{\text{tolyl}_2\text{Al}_3\text{Me}_5}$, and $\text{D}^{\text{ph}_2\text{Al}_3\text{Me}_5}$ are soluble in CDCl_3 . The ^1H NMR peaks of the two methine groups of $\text{D}^{\text{Ad}_2\text{Al}_3\text{Me}_5}$, $\text{D}^{\text{Pr}_2\text{Al}_3\text{Me}_5}$, $\text{D}^{\text{tolyl}_2\text{Al}_3\text{Me}_5}$, and $\text{D}^{\text{ph}_2\text{Al}_3\text{Me}_5}$ were at 6.37, 6.42, 6.45, and 6.58 ppm, respectively, and three sets of methyl groups with a 2:2:1 integration were also observed (Figures S8 and S9).

The molecular structure of $\text{D}^{\text{Bu}_2\text{Al}_3\text{Me}_5}$ (Figure 2) was characterized using a single-crystal X-ray diffraction analysis (CCDC 1955471). The external Al atoms on each side exhibited a distorted-tetrahedral geometry due to their association with two methyl groups. The central Al atom has a quadrangular-pyramidal geometry with one methyl group and four nitrogen atoms, one from each of the four pyrazolidyl groups. Surprisingly, the Al–C bonds of the pentacoordinated central Al atom were shorter than those of tetracoordinated Al atoms on either side of the complex (Table S35).

Polymerization of ϵ -Caprolactone. The results of the catalytic activity for CL polymerization in toluene in the presence of benzyl alcohol (BnOH) are presented in Table 1. The optimization of CL polymerization using $\text{D}^{\text{Bu}_2\text{Al}_3\text{Me}_5}$ as a catalyst with BnOH was investigated as shown in entries 1–3 of Table 1, and the optimal $[\text{D}^{\text{Bu}_2\text{Al}_3\text{Me}_5}]:[\text{BnOH}]$ ratio was 1:5 with the greatest catalytic activity and controllability. In comparison with $\text{L}^{\text{Bu}_2\text{Al}_2\text{Me}_4}$, $\text{D}^{\text{Bu}_2\text{Al}_3\text{Me}_5}$ had a substantially higher catalytic activity for CL polymerization ($[\text{CL}]:[\text{D}^{\text{Bu}_2\text{Al}_3\text{Me}_5}]:[\text{BnOH}] = 100:0.5:2.5$, where $[\text{CL}] = 2 \text{ M}$, conversion 93% at 25°C after 18 min; entry 2 in Table 2). The k_{obs} value of $\text{D}^{\text{Bu}_2\text{Al}_3\text{Me}_5}$ is 16 times higher than that of $\text{L}^{\text{Bu}_2\text{Al}_2\text{Me}_4}$. Similarly, in a comparison of $\text{D}^{\text{ph}_2\text{Al}_3\text{Me}_5}$ and $\text{L}^{\text{ph}_2\text{Al}_2\text{Me}_4}$, the k_{obs} value of $\text{D}^{\text{ph}_2\text{Al}_3\text{Me}_5}$ was determined to be twice that of $\text{L}^{\text{ph}_2\text{Al}_2\text{Me}_4}$, further demonstrating that trinuclear Al complexes have greater catalytic activity than do dinuclear Al complexes. In addition, phenyl and tolyl groups on the 5,5'-positions of bipyrazoles reduced the catalytic activity of

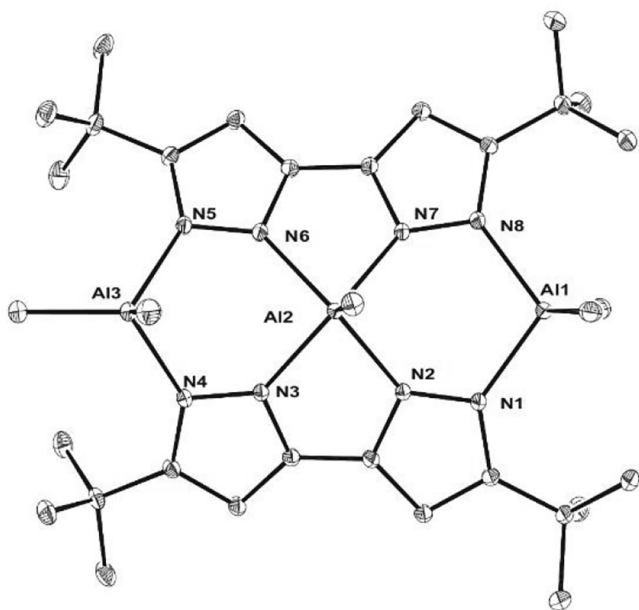


Figure 2. Molecular structure of $D^{Bu}_2Al_3Me_5$ depicted as 20% probability ellipsoids. All of the hydrogen atoms are omitted for clarity. The selected bond lengths (Å) of Al(1)–C(1), Al(1)–C(2), Al(2)–C(3), Al(3)–C(4), and Al(3)–C(5) are 1.960(3), 1.969(3), 1.942(3), 1.974(3), and 1.960(3), respectively. The selected bond angles (deg) of C(1)–Al(1)–C(2), C(4)–Al(3)–C(5), N(1)–Al(1)–N(8), N(4)–Al(3)–N(5), N(2)–Al(2)–N(7), N(7)–Al(2)–N(6), N(6)–Al(2)–N(3), and N(3)–Al(2)–N(2) are 123.96(12), 109.30(13), 106.01(8), 99.55(8), 89.85(8), 80.36(8), 88.19(8), and 80.32(8), respectively.

trinuclear Al complexes in comparison with that of $D^{Bu}_2Al_3Me_5$. Moreover, the catalytic activity of $L^{Ad}_2Al_2Me_4$ was greater than those of $L^{Bu}_2Al_2Me_4$ and $L^{Pr}_2Al_2Me_4$, and this revealed that increasing the steric bulk of the groups on the

5,5'-positions of ligands can enhance the catalytic activity of CL polymerization. The reason was discussed in a mechanism study. When the linear relationship between $M_{n,GPC}$ and $([monomer]_0 \times conversion)/[BnOH]$ (entries 3, 4, and 11–15 in Table 1) presented in Figure 3 was considered, $D^{Bu}_2Al_3Me_5$ as a catalyst was deemed to be highly controllable and to have acceptable polydispersity indexes (\mathcal{D} s) for CL polymerization. However, Figure 3 also revealed that only two to three BnOHs could be initiators to initiate CL. This may be ascribed to two bulky tBu groups restraining the two benzyl alkoxide exchanges and prevent BnOH in a far position from attacking CL.

To examine the living and immortal properties^{19,52–60} of $D^{Bu}_2Al_3Me_5$ in CL polymerization, 25 equiv of BnOH was combined with 200 equiv of CL in 5 mL of toluene. After >90% conversion, 50 equiv of CL monomers was reloaded into the solution. This step was repeated until the solution could not be stirred. The solution could not be stirred after 17 additions of CL (total ratio $[CL]:[D^{Bu}_2Al_3Me_5]:[BnOH] = 1050:1:25$; Table 2 and Figure 4). The results revealed that $D^{Bu}_2Al_3Me_5$ had excellent living and immortal properties in CL polymerization. In addition, the results also revealed that at least four-fifths of BnOH can participate in the ring-opening polymerization reaction. This proved that the free alcohol could easily exchange with the alkoxide on an Al atom to form a new alkoxide to initiate CL.

Kinetic Study of ϵ -Caprolactone Polymerization. The kinetic data (Table S2 and Figures S2 and S3) revealed that the polymerization rate had a first-order dependence on the monomer concentration. In CL polymerization, the k_{obs} value of $D^{Bu}_2Al_3Me_5$ was 0.188 min^{-1} , and the polymerization rate was 15 times higher than that associated with $L^{Bu}_2Al_2Me_4$ (0.0123 min^{-1}). After k_{obs} was plotted against $[D^{Bu}_2Al_3Me_5 \cdot 5BnOH]$ ($[D^{Bu}_2Al_3Me_5 \cdot 5BnOH]$ being a mixture of 1 equiv of $D^{Bu}_2Al_3Me_5$ with 5 equiv of BnOH), the k_{prop} (propagation) value was calculated to be 15.01 (Figure S3). CL polymer-

Table 1. ϵ -Caprolactone Polymerization with Al Complexes as Catalysts^a

entry	cat.; [CL]:[cat.]:[BnOH]	time (min)	conversn (%) ^b	$M_{n,Cal}$ ^b	$M_{n,NMR}$ ^c	$M_{n,GPC}$ ^d	\mathcal{D}^d	k_{obs} (error), 10^3 min^{-1}
1 ^e	$D^{Bu}_2Al_3Me_5$; 100:1:1	240	93	10700	19400	19500	1.35	8.8 (1)
2 ^f	$D^{Bu}_2Al_3Me_5$; 100:1:3	35	90	3500	5600	6400	1.52	67.5 (1)
3 ^g	$D^{Bu}_2Al_3Me_5$; 100:1:5	12	95	2300	3500	3600	1.24	283.0 (16)
4 ^a	$D^{Bu}_2Al_3Me_5$; 100:0.5:2.5	18	93	4300	8200	8700	1.30	188.1 (32)
5 ^a	$L^{Bu}_2Al_2Me_4$; 100:0.5:2	250	93	5400	7400	7900	1.13	12.3 (4)
6 ^a	$D^{Ad}_2Al_3Me_5$; 100:0.5:2.5	16	92	4300	7300	6400	1.24	205.0 (30)
7 ^a	$D^{Pr}_2Al_3Me_5$; 100:0.5:2.5	60	90	4200	5300	5900	1.11	52.5 (1)
8 ^a	$D^{Ph}_2Al_3Me_5$; 100:0.5:2.5	55	90	4200	6200	5200	1.14	57.1 (1)
9 ^a	$L^{Ph}_2Al_2Me_4$; 100:0.5:2	100	90	5200	5500	7000	1.34	26.2 (4)
10 ^a	$D^{tolyl}_2Al_3Me_5$; 100:0.5:2.5	55	90	4200	5900	4600	1.10	52.8 (1)
11 ^h	$D^{Bu}_2Al_3Me_5$; 100:0.75:3.75	15	90	2800	5800	5300	1.27	204.6 (33)
12 ⁱ	$D^{Bu}_2Al_3Me_5$; 100:0.25:1.25	70	90	8300	15300	15300	1.29	38.2 (9)
13 ^j	$D^{Bu}_2Al_3Me_5$; 200:1:5	20	96	4500	8300	9000	1.25	<i>m</i>
14 ^k	$D^{Bu}_2Al_3Me_5$; 400:1:5	58	97	9200	14100	16300	1.29	<i>m</i>
15 ^l	$D^{Bu}_2Al_3Me_5$; 500:1:5	75	98	11300	22300	26000	1.28	<i>m</i>

^aUnless specified otherwise, the reaction was carried out in toluene with $[CL] = 2 \text{ M}$, $[CL]:[Cat.]:[BnOH] = 100:0.5:2.5$, at 25 °C for entries 1, 3, and 5, and $[CL]:[Cat.]:[BnOH] = 100:0.5:2$ for entries 2 and 4). ^bCalculated from the molecular weight of $M_w(CL) \times [CL]_0/[BnOH]_0 \times conversion \text{ yield} + M_w(BnOH)$. ^cThe data were determined using ¹H NMR analysis. ^dObtained through gel permeation chromatography (GPC). Values of $M_{n,GPC}$ were obtained times 0.56 for PCL. ^eThe $[CL]:[Cat.]:[BnOH]$ ratio is 100:1:1 in toluene with $[CL] = 2 \text{ M}$. ^fThe $[CL]:[Cat.]:[BnOH]$ ratio is 100:1:3 in toluene with $[CL] = 2 \text{ M}$. ^gThe $[CL]:[Cat.]:[BnOH]$ ratio is 100:1:5 in toluene with $[CL] = 2 \text{ M}$. ^hThe $[CL]:[Cat.]:[BnOH]$ ratio is 100:0.75:3.75 in toluene with $[CL] = 2 \text{ M}$. ⁱThe $[CL]:[Cat.]:[BnOH]$ ratio is 100:0.25:1.25 in toluene with $[CL] = 2 \text{ M}$. ^jThe $[CL]:[Cat.]:[BnOH]$ ratio is 200:1:5 in toluene with $[CL] = 4 \text{ M}$. ^kThe $[CL]:[Cat.]:[BnOH]$ ratio is 400:1:5 in toluene with $[CL] = 7 \text{ M}$. ^lThe $[CL]:[Cat.]:[BnOH]$ ratio is 500:1:5 in toluene with $[CL] = 10 \text{ M}$. ^mDid not study.

Table 2. CL Polymerization with $D^{Bu}_2Al_3Me_5$ for Living and Immortal Characters^a

entry	[CL]:[$D^{Bu}_2Al_3Me_5$]:[BnOH]	time (min)	conversn ^b (%)	$M_{n,Cal}$ ^c	$M_{n,GPC}$ ^d	$M_{n,NMR}$ ^e	D^d
1	200:1:25	36	93	1000	900	1500	1.11
2	250:1:25	47	95	1200	1000	1700	1.15
3	300:1:5	58	90	1300	1200	1800	1.13
4	350:1:25	75	93	1600	1500	2200	1.12
5	400:1:25	90	92	1800	1600	2500	1.14
6	450:1:25	105	93	2000	1900	2800	1.15
7	500:1:25	121	91	2200	2100	3300	1.18
8	550:1:25	135	92	2400	2200	3600	1.19
9	600:1:25	156	92	2600	2600	3800	1.21
10	650:1:25	172	93	2900	2800	4000	1.21
11	700:1:25	195	92	3000	3000	4300	1.23
12	750:1:25	218	92	3300	3200	4500	1.26
13	800:1:25	249	92	3500	3400	4700	1.27
14	850:1:25	280	95	3800	3600	4900	1.25
15	900:1:25	320	92	3900	3800	5200	1.23
16	950:1:25	380	95	4200	4200	5400	1.27
17	1000:1:25	450	93	4300	4300	5600	1.27
18	1050:1:25	540	90	4400	4600	5900	1.27

^aAdd 50 equiv of CL in comparison with [$D^{Bu}_2Al_3Me_5$] in every entry. ^bIn general, the reaction was carried out in toluene with [$D^{Bu}_2Al_3Me_5$] = 0.02 M at 25 °C. ^cCalculated from the molecular weight of $M_w(CL) \times [CL]_0/[BnOH]_0 \times$ conversion yield + $M_w(BnOH)$. ^dValues of $M_{n,GPC}$ were those from GPC times 0.56. ^eThe data were determined from ¹H NMR analysis.

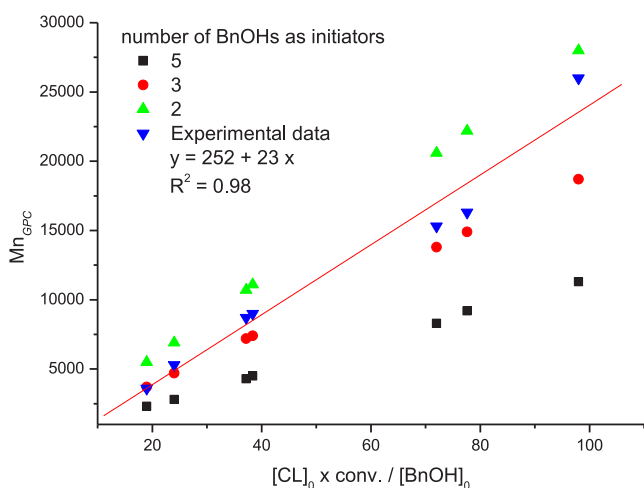


Figure 3. Linear plots of $M_{n,GPC}$ versus $([CL]_0 \times \text{conversion})/[BnOH]$, (blue inverted triangles \blacktriangledown , entries 3, 4 and 11–15) in Table 2. Black squares \blacksquare are theoretical values calculated with 5 equiv of BnOHs as initiator, red dots \bullet indicate 3 equiv of BnOH, and green triangles \blacktriangle indicate 2 equiv of BnOH.

ization with $D^{Bu}_2Al_3Me_5$ as the catalyst exhibited the following rate law:

$$d[CL]/dt = 15.01 \times [CL][D^{Bu}_2Al_3Me_5 \cdot 5BnOH]$$

Dinuclear Al complexes bearing pyrazole exhibited a high catalytic activity in CL ROP because of electronic and dinuclear cooperative effects between the two Al atoms,²⁹ with the Al–Al distance being 3.525–3.783 Å. In $D^{Bu}_2Al_3Me_5$, the distance between the central Al(2) and the external Al(1) was 3.785 Å and the Al(2)–Al(3) distance was 3.662 Å, suggesting that trinuclear cooperation influenced polymerization in the $D^{Bu}_2Al_3Me_5$ system. In addition, in comparison with the dinuclear Al complex $L^{Bu}_2Al_2Me_4$, the trinuclear Al complex $D^{Bu}_2Al_3Me_5$ had a stronger electronic effect (Al^{3+} – Al^{3+} charge influence, which comes from the direct electron-

withdrawing effect of the external Al to the central Al via bridging pyrazole ligands described below). Thus, a higher catalytic activity for CL polymerization was observed.

Density Functional Theory Analysis of the CL Polymerization Mechanism Study Using $D^{Bu}_2Al_3Me_5$ as a Catalyst. The reaction mechanism, as shown in Figures 5 and 6, was studied using density functional theory (DFT) at the B3LYP/6-31G(d) level. The values of the free energies obtained from the DFT calculation results are shown in Figure 7. In the mechanism study, all of the methyl groups on Al atoms of $D^{Bu}_2Al_3Me_5$ were replaced by MeO^- ligands to form $D^{Bu}_2Al_3(OMe)_5$ (cat) because all methyl groups on Al atoms of $D^{Bu}_2Al_3Me_5$ are strong bases and can be readily replaced by alcohol molecules under the reaction conditions.

To better understand the activity of the catalysts, the Mulliken charges of the Al atoms of $D^{Bu}_2Al_3Me_5$ and $L_2Al_2Me_4$ were calculated on the basis of their crystal structures, as shown in Figure 8. The charges of the two Al atoms of $L_2Al_2Me_4$ were both calculated to be +0.8517, and the charges of the central and the external Al atoms of $D^{Bu}_2Al_3Me_5$ were calculated to be +0.929 and +0.836 (average), respectively. Therefore, the central Al of $D^{Bu}_2Al_3Me_5$ has much higher Lewis acidity than do the external Al atoms of $L_2Al_2Me_4$. Therefore, CL molecules can be attracted by the central Al of $D^{Bu}_2Al_3Me_5$, increasing the effective concentration for CL coordination and reactivity.

After $D^{Bu}_2Al_3Me_5$ reacts with the initiator alcohol to form cat, three sets of MeO^- ligands located in totally different environments on cat can be found. The first set is one MeO^- ligand pointing up on the central Al atom. The second is two MeO^- ligands pointing up on the two external Al atoms (one on each). The third is two MeO^- ligands pointing down on the two external Al atoms (one on each). Because the rigid bipyrazole ligands on cat prohibit the formation of bridged methoxide structures (the average Al...Al distance is 3.779 Å, which is longer than 2 times the length of Al–OMe bonds, about 3.4 Å), the anionic MeO^- ligand cannot migrate among Al atoms without breaking strong O–Al coordination bonds.

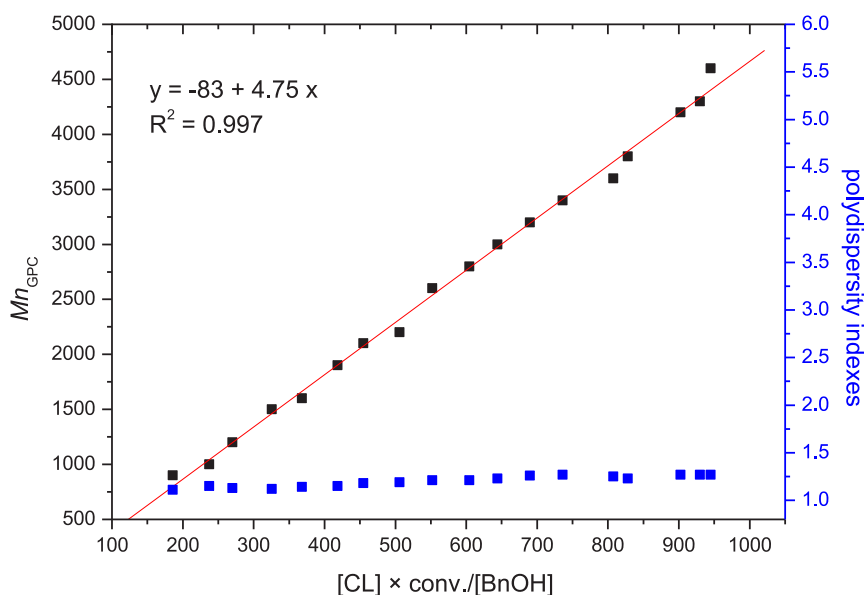


Figure 4. Linear plot of $M_{n,GPC}$ vs $[CL]_0 \times \text{conversion}/[BnOH]$, with D indicated by blue squares ■.

Moreover, due to the restricted and crowded coordination environment around external Al, the structure distortions are impossible. The rigid N–Al–N angle (105° , average) and the small distances (about 4 Å, average) between H atoms of the two ^tBu groups both restrict the relocation of the Al atom and two MeO[−] ligands to form an SP geometry. This results in the fact that the two MeO[−] ligands are structurally isolated, and therefore the interchange is hindered. This can explain why only the two alkoxide ligands close to the CL receiving site are active in the polymerization reaction. However, if free alcohols are present in the system, ligand exchange processes assisted by those free alcohols become a possible pathway to increase the number of alkoxide ligands involved in the catalytic reaction.

In the catalytic cycle study of the first mechanism (right part of Figure 5), the calculation results demonstrate that a CL molecule first approached the central Al atom to form intermediate I (Figure 9) with a free energy of 7.81 kcal mol^{−1}. The structure of I is similar to those of $D^{Bu}_2Al_3Me_3$ and **cat**, except for the central Al, which has a distorted-octahedral structure. The distance between the CL carbonyl O and the central Al is 2.983 Å, which is longer than the sum of the single bond covalent radii of O and Al (1.89 Å)⁶² but shorter than the sum of the crystallographic van der Waals radii of O and Al (3.65 Å).⁶³ This indicates that the CL carbonyl O does not directly coordinate to the central Al but is attracted by noncovalent interactions. However, the distance between the α -hydrogen pointing toward the plane of the complex and the pyrazole ring is 2.901 Å, which is in the range of a C–H $\cdots\pi$ interaction.⁶⁴ The central Al intrudes into the plane formed by the four coordinated N atoms toward the MeO[−] ligand. The distance between the Al atom and the plane is 0.494 Å, which is slightly shorter than that of $D^{Bu}_2Al_3Me_3$ (0.604 Å) due to the interaction between the CL carbonyl O and the central Al. The average bond length of the four N–Al bonds of the central Al is 1.990 Å, which is slightly longer than that of the external Al atoms (1.965 Å).

In intermediate I, the CL molecule is captured onto the pentacoordinate central Al by two noncovalent interactions to increase the effective concentration of CL in **cat**. Moreover, the relatively weak noncovalent interactions allow CL to be

transferred readily from the trap site to the reaction site. For these reasons, this capturing phenomenon can dramatically increase the collision frequency between CL molecules and a MeO[−] initiator to increase the reaction rate. Moreover, because of those two interactions, the sp² plane of the CL ester group is locked, facing one MeO[−] ligand on the external Al. This conformation locking increases the ratio of effective collision overall, facilitating the addition of the MeO[−] ligand to the ester group of CL. These are the primary effects promoting the catalytic activity of the trinuclear complex.

The CL molecule on the central Al moves toward the MeO[−] ligand on one external Al. The addition of MeO[−] to the carbonyl C goes through transition state 1 (TS1). The free energy of TS1 is 28.7 kcal mol^{−1}, and the energy barrier for this reaction is 20.89 kcal mol^{−1}. This is a reasonable energy barrier for room-temperature reactions.⁶¹ On consideration of the high effective concentration of CL on **cat** and high effective collision rate, the overall reaction rate is expected to be high. In the transition structure, the distance between the CL carbonyl O and the central Al is 3.716 Å, and the distance between the carbonyl O and the closer external Al is 1.941 Å, implying that the central Al plays a role in monomer capture but does not directly cooperate with the external Al to activate the CL carbonyl group. The distance between the CL carbonyl C and the methoxy O atom is 1.905 Å. The distance between the methoxy O and the external Al is 1.912 Å. The distance between the CL carbonyl O and the external Al is 1.941 Å. After a transition, the central Al returns to a pentacoordinate structure with a square-pyramidal geometry.

After MeO[−] insertion to CL, intermediate II is formed. This intermediate has a free energy of 11.87 kcal mol^{−1}. The structure of II resembles that of **cat** with one pentacoordinated central Al atom and two tetraordinated external Al atoms. The distance between the CL–MeO adduct alkoxy O atom and the Al atom on which it coordinates is 1.752 Å. This distance is slightly longer than the lengths of the other three O–Al bonds on the two external Al atoms (average: 1.718 Å) and that of the central Al (1.734 Å). The longer Al–O bond between the CL–MeO adduct and Al is expected to be caused by the repulsion between the bulky structure of the adduct and the

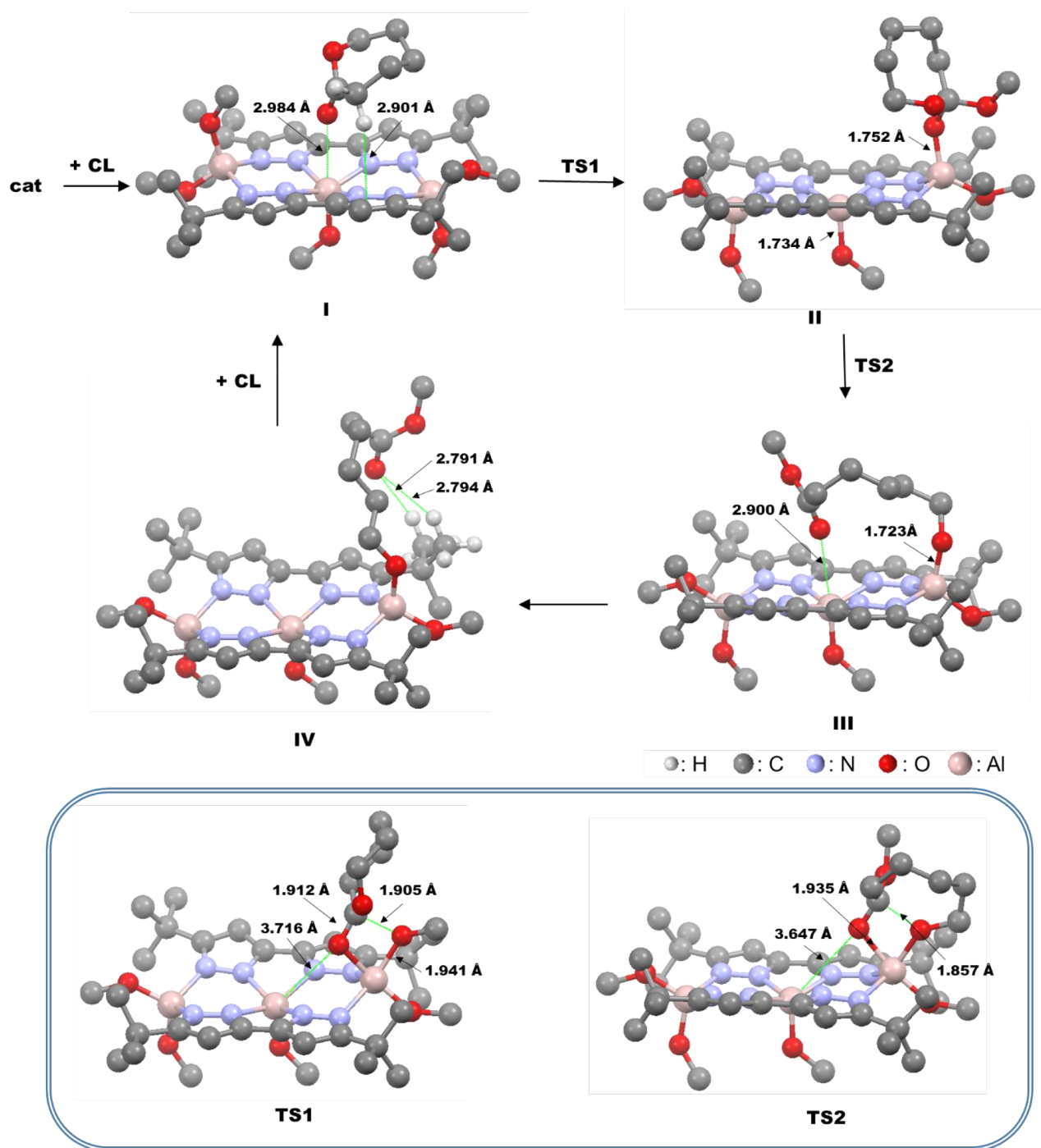


Figure 5. First reaction mechanism of ring-opening polymerization of CL catalyzed by $D^{Bu}_2Al_3(OMe)_5$.

two *t*-Bu groups on the ligands. This is one of the driving forces for the next step in the catalytic cycle reaction opening the CL ring.

The CL ring opens through transition state 2 (TS2). This transition structure has a free energy of $33.42 \text{ kcal mol}^{-1}$, and the energy barrier for this reaction is $21.55 \text{ kcal mol}^{-1}$. Although this energy barrier is slightly higher than that of the reaction through TS1, the intramolecular characteristic of this reaction causes this step to be more favorable than the step through TS1. In this transition structure, the newly formed carbonyl group migrates from the external Al to the central Al and the C–O bond in the CL ring breaks. The distance

between the newly formed carbonyl O atom and the central Al atom is 3.647 \AA , and the distance between the newly formed carbonyl O atom and the external Al atom is 1.935 \AA . These distances are both shorter than those of TS1, indicating that after the CL ring is opened, due to a decrease in steric repulsion, the carbonyl group can be more easily attracted by the two Al atoms. The distance between the newly formed carbonyl C atom and the newly formed alkoxy O atom is 1.857 \AA , which is shorter than that of TS1, indicating that the structure of TS2 is relatively close to that of intermediate II in comparison to the structures between intermediate II and TS1. Interestingly, the steric repulsion also is one important driving

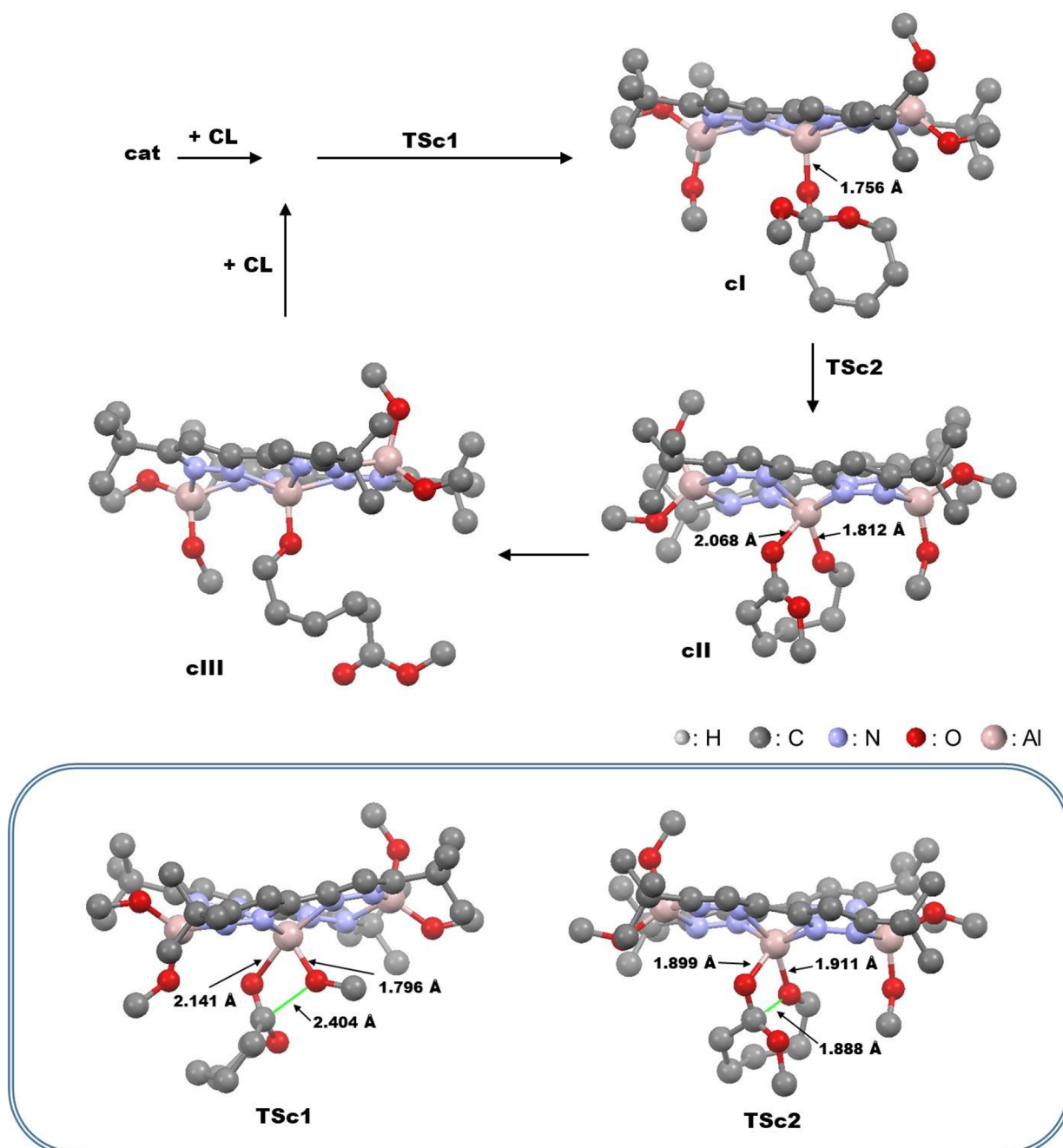


Figure 6. Second reaction mechanism of ring-opening polymerization of CL catalyzed by $D^{Bu_2}Al_3(OMe)_5$.

force to assist in CL ring opening. In the structure of TS2, the shortest distance between the H atoms of t Bu groups and those of the CL ring is 2.451 Å, which is close to the closest possible distance between two isolated H atoms from the point of view of van der Waals radii.⁶³ Together with thermal motion, these two groups shall collide at high frequency to introduce a large repulsion force between them to assist CL ring opening.

After the CL ring opens, intermediate III is formed when the newly formed carbonyl group coordinates with the central Al atom to form a hexacoordinate structure. The free energy of intermediate III is 6.97 kcal mol⁻¹, which is lower than that of intermediate I. The newly formed alkoxy O atom is bonded to the external Al atom, and the newly formed carbonyl O atom is bonded to the central Al atom. The distance between the

newly formed carbonyl O atom and the central Al atom is 2.900 Å, which is slightly shorter than that of intermediate I due to the less bulky structure of the opened CL chain. The bond length between the external Al atom and the alkoxy O atom of the opened CL is 1.723 Å. The central Al atom also intrudes toward the MeO⁻ ligand with a distance of 0.482 Å from the central NNNN plane of intermediate III, but the distance is slightly shorter than that of intermediate I, because of the stronger carbonyl O–Al interaction in intermediate III than in intermediate I.

Finally, the carbonyl O atom of the opened CL leaves the central Al atom to form intermediate IV. The free energy of intermediate IV, 6.11 kcal mol⁻¹, is slightly lower than that of intermediate III. The structure of IV is almost identical with

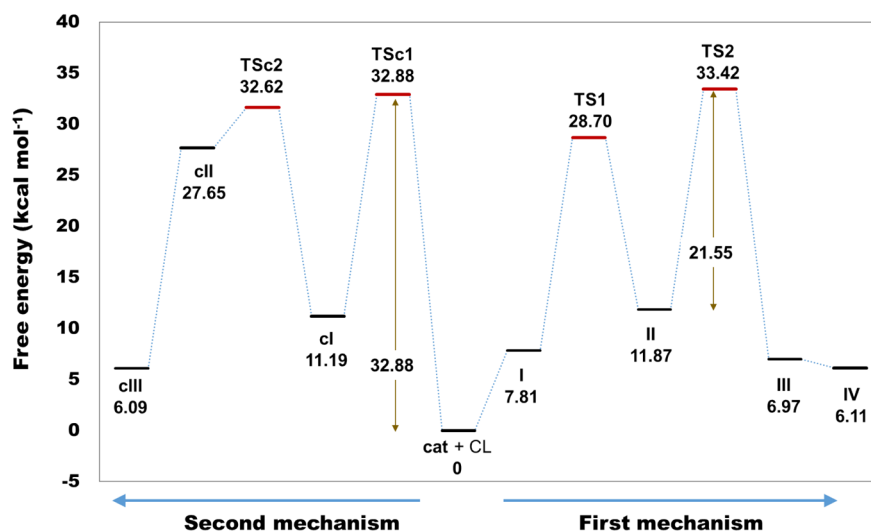


Figure 7. Energy diagram of all the intermediates and transition structures. The sum of free energies of cat and CL is set as 0 kcal mol⁻¹.

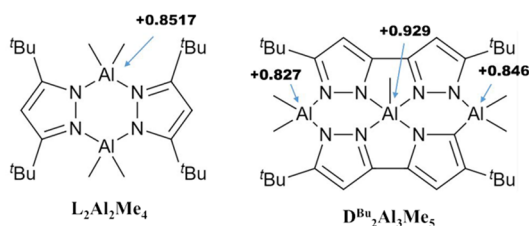


Figure 8. Mulliken charges of Al atoms in $L_2Al_2Me_4$ and $D_2Al_2Me_5$.

that of cat. The newly formed carbonyl group moves from the central Al atom toward the ^tBu groups of the bipyrazole ligand. The distances between the carbonyl O atom and the closest two H atoms on the ^tBu groups are 2.794 and 2.791 Å. These distances are close to the sum of the crystallographic van der Waals radii (~2.75 Å) but are smaller than the sum of the equilibrium van der Waals radii (~3 Å), indicating that the ^tBu groups weakly attract the carbonyl group, assisting in its detachment from the central Al.

Another possible catalytic reaction cycle proceeds entirely on the central Al atom, as shown in the left side of Figure 5. A CL molecule approaches the central Al atom from the direction of the MeO⁻ ligand to directly form transition structure c1 (TSc1) without forming a CL-coordinated intermediate. No stable CL-coordinated intermediate has been found in the calculations even when the structural search is carried out from TSc1 to elongate the length between the carbonyl C atom and the methoxy group. In this transition

structure, the central Al atom is farther from the NNNN plane with a distance of 0.828 Å, forming a highly distorted hexacoordinated structure. The distance between the carbonyl O atom and central Al atom is 2.141 Å. The distance between the CL carbonyl C atom and central Al methoxy O atom is 2.404 Å much longer than that of TS1. The distance between the methoxy O atom and central Al atom is 1.796 Å. These structural characteristics are more similar to CL-coordinated intermediates than to transition structures because C–O bond formation and the central Al atom distortion process are coupled in this step. Distorting the geometry of the central Al atom requires substantially more energy than that required for overcoming the C–O bond formation in this step.

After TSc1, intermediate cI, in which the CL–MeO adduct coordinates on the central Al atom, is formed. The free energy of intermediate cI is 11.19 kcal mol⁻¹, which is slightly lower than that of intermediate II because the less crowded environment of the central Al is less crowded. This structure resembles the structure of cat and intermediate II, with a pentacoordinated central Al atom and two tetracoordinated external Al atoms. The distance between the central Al and the alkoxy O atom of the CL–MeO adduct is 1.756 Å. The distance between the central Al and the NNNN plane is 0.584 Å, indicating that the Al returns to a stable coordination position in this complex.

The CL ring then opens through transition state c2 (TSc2). The free energy of TSc2 is 31.62 kcal mol⁻¹, and the energy barrier of this reaction step is 20.43 kcal mol⁻¹. This energy

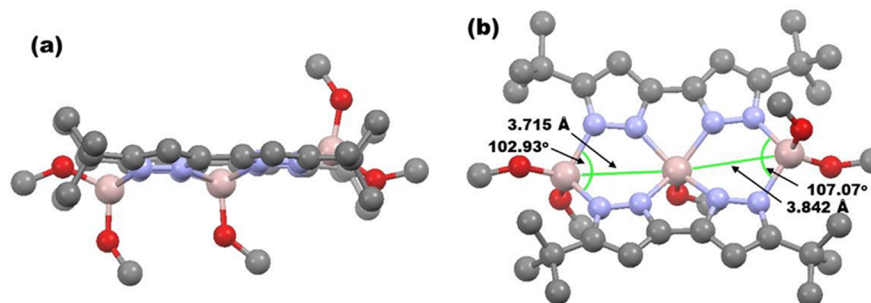


Figure 9. Side-view structure (a) and top-view structure (b) of cat.

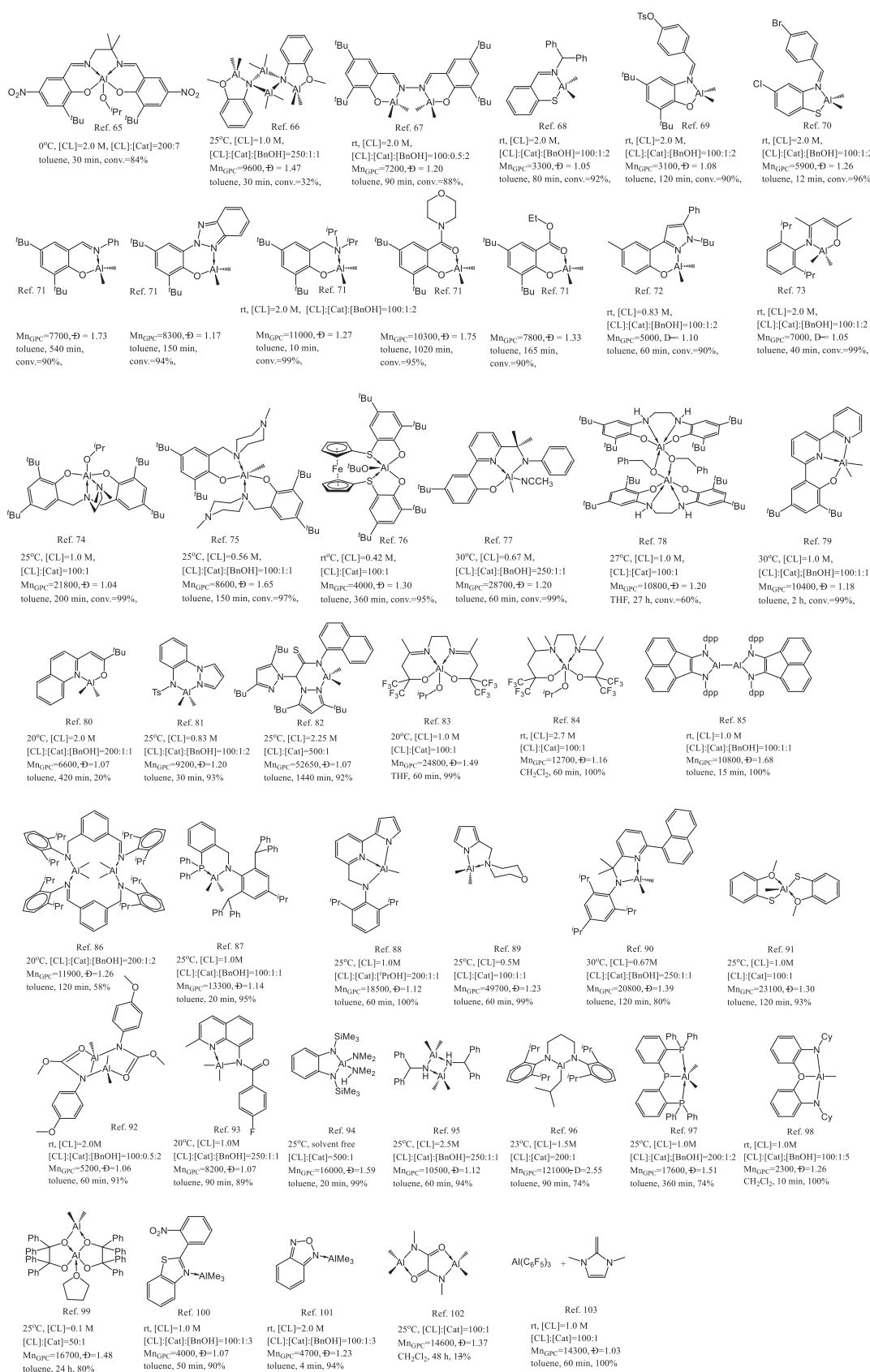


Figure 10. Survey of the recent literature sources on CL polymerization using Al complexes at 0–30 °C.

barrier is similar to that of TS2 in the first mechanism. In this transition structure, the central Al atom (resembling that of TS1) retreats from the NNNN plane to a distance of 0.830 Å.

The distance between the newly formed carbonyl O atom and the central Al atom is 1.899 Å. The distance between the newly formed alkoxy O atom and the central Al atom is 1.911 Å. The

length of the broken C–O bond in the CL ring is 1.888 Å. This bond is very similar to those of TS1 and TS2, indicating that this transition structure is dominated by the breaking of the O–C bond of CL.

After the breakage of the C–O bond in the CL ring, intermediate cIII is formed, in which the newly formed carbonyl group is still coordinated on the central Al. The free energy of cIII is 27.65 kcal mol⁻¹, substantially higher than those of other intermediates and closer to those of the transition structures. The increased energy is because the central Al atom is still in a highly distorted geometry. The distance between the newly formed carbonyl O atom and the central Al atom is 2.068 Å. The distance between the newly formed alkoxy O atom and the central Al atom is 1.812 Å. The distance between the central Al atom and the NNNN plane is 0.846 Å.

Finally, the carbonyl group of the opened CL chain is detached from the central Al atom to form intermediate cIII, closing this catalytic cycle. The structure of intermediate cIII is almost identical with those of cat and intermediate IV. The free energy of intermediate cIII is 6.09 kcal mol⁻¹, which is much lower than the free energy of cII but close to that of IV.

On the basis of our calculated results, the first catalytic cycle is considered the most likely mechanism for the CL ROP reaction. First, the highest energy barrier of the first mechanism is 21.55 kcal mol⁻¹ (II to III through TS2) and that of the most difficult reaction step (I to II through TS1) is 20.89 kcal mol⁻¹; these energy barriers are much lower than those of the second mechanism (32.88 kcal mol⁻¹ for the step from cat and CL to intermediate cI through TS1). Second, the effective concentration of CL is substantially increased in the first mechanism due to the monomer capture effect of the central Al atom on the base side of the square-pyramidal structure. Third, the two noncovalent interactions create a special conformational lock effect on CL, increasing the effective collision rate between CL and MeO⁻. Fourth, the bulky ^tBu groups around the external Al atom effectively assist in the ring opening of CL (TS2).

Comparison of CL Polymerization in the Literature. A survey of recent literature of CL polymerization using Al complexes as catalysts at 0–30 °C is illustrated in Figure 10. An Al complex bearing a Salen ligand⁶⁵ revealed the greatest catalytic activity in CL polymerization at 0 °C. Other Al complexes, including an Al complex⁷¹ bearing aminophenolate, a low-valent Al(II)–Al(II) complex⁸⁵ bearing 1,2-bis(2,6-*i*Pr₂-C₆H₃)-iminoaceneaphthene, an Al complex⁹⁸ bearing (oxybis-(2,1-phenylene))bis(cyclohexylamide), a five-membered Al complex⁷⁰ bearing a thiol-Schiff base, and an Al complex¹⁰¹ bearing benzofurazan, as well as D^{Bu}₂Al₃Me₅ could polymerize CL in 15 min at room temperature. In comparison with these Al complexes in Figure 10, the collaboration that each Al atom performs its own functions can indeed effectively improve the catalytic activity of the Al catalyst.

CONCLUSIONS

A series of trinuclear Al complexes bearing bipyrazoles were synthesized, and their CL polymerization rates were studied. The trinuclear Al complexes had a substantially higher (2–15 times higher *k*_{obs} value) CL polymerization rate. DFT calculations revealed that the reaction is a cooperated bimetal catalytic reaction between the pentacoordinated central Al atom and the tetracoordinated external Al atom. The reactivity is improved due to an increased effective concentration of CL

and the conformation lock effect induced by weak interactions generated by the central Al atom and the π-system of ligands.

EXPERIMENTAL SECTION

Standard Schlenk techniques and a N₂-filled glovebox were used throughout the isolation and handling of all the compounds. Solvents, ε-caprolactone, and deuterated solvents were purified prior to use. Deuterated chloroform and ε-caprolactone were purchased from Acros. Benzyl alcohol, trimethylaluminum, *tert*-butyl methyl ketone, diethyl oxalate, methyl phenyl ketone, methyl *p*-tolyl ketone, 4'-chloroacetophenone, 4'-bromoacetophenone, and hydrazine hydrate were purchased from SIGMA-Aldrich. ¹H and ¹³C NMR spectra were recorded on a Varian Gemini2000-200 (200 MHz for ¹H and 50 MHz for ¹³C) spectrometer with chemical shifts given in ppm from the internal TMS or the center line of CDCl₃. Microanalyses were performed using a Heraeus CHN-O-RAPID instrument. GPC measurements were performed on a Jasco PU-2080 PLUS HPLC pump system equipped with a differential Jasco RI-2031 PLUS refractive index detector using THF (HPLC grade) as an eluent (flow rate 1.0 mL/min, at 40 °C). The chromatographic column was JORDI Gel DVB 10³ Å, and the calibration curve was made by primary polystyrene standards to calculate *M*_{n,GPC}. All single-crystal X-ray diffraction data were accumulated using Rigaku Oxford Diffraction single-crystal X-ray diffractometers with Mo Kα radiation (λ = 0.71073 Å). The data collection was executed using the CrysAlisPro 1.171.41.56a program. Cell refinement and data reduction were carried out with the CrysAlisPro 1.171.41.56a program. The structure was determined using the Olex2/ShellXL program refined using full-matrix least squares. All non-hydrogen atoms were refined anisotropically, whereas hydrogen atoms were placed at calculated positions and included in final stage of refinement with fixed parameters. D^{Bu}-H,¹⁰⁴ D^{Ph}-H,⁵⁰ D^{tolyl}-H,⁵⁰ and D^{Cl}-H⁵⁰ were prepared following the literature procedures.

Synthesis of D^{Br}-H. To a solution of sodium hydride (1.04 g, 0.052 mol) in dry THF was slowly added a THF solution of 4'-chloroacetophenone (4.2 g, 0.0208 mol) at room temperature, and the mixture was heated to 50 °C. The reaction mixture was stirred for 1 h and a THF solution of diethyl oxalate (1.53 g, 0.0104 mol) added slowly for 1 h at 50 °C. The reaction mixture was stirred overnight and quenched with cold water at room temperature. The aqueous layer was separated and the pH adjusted to 3–4 using a 2 N HCl solution and extracted with diethyl ether (3 × 50 mL). The combined organic layers were washed with brine solution and dried over magnesium sulfate. The organic layer was concentrated and the crude 1,6-diphenylhexane-1,3,4,6-tetraone (3.25 g, 35%) obtained was used as such in the next step. To a solution of 0.003 mol of an appropriate 1,3,4,6-tetraketone (1.33 g, 0.003 mol) in ethanol (10 mL) was added 1 mL (excess) of a 70% water solution of hydrazine, and the mixture was boiled for 4 h. The precipitate obtained was filtered and washed with ethanol (2 mL) and diethyl ether. The product was dried to give the product as a white solid. Yield: 0.61 g (46%). ¹H NMR (DMSO-*d*₆, 400 MHz): δ 7.74 (d, *J* = 8.0 Hz, 4H, *m*-Br-PhH), 7.55 (d, *J* = 8.0 Hz, 4H, *o*-Br-PhH), 6.806 (s, 2H, Pz-H). ¹³C NMR (CDCl₃, 400 MHz): δ 148.57 (Ar-C^{Pz}), 144.43 (Pz-C^{Pz}), 133.43, 131.58, 127.07, 120.09 (C^{Ar}), 102.80 (H-C^{Pz}). Anal. Calcd (found) for C₁₈H₁₂Br₂N₄: C, 48.68 (48.55); H, 2.72 (2.65); N, 12.62 (12.50).

Synthesis of D^{Pr}-H. This compound was obtained using a method similar to that for D^{Br}-H except methyl 2-butanone was used in place of 4'-chloroacetophenone. Yield: 2.1 g (60%). ¹H NMR (DMSO-*d*₆, 400 MHz): δ 6.22 (s, 2H, Pz-H), 2.91 (br, 2H, Me₂CH), 1.19 (d, 12H, (CH₃)₂CH). ¹³C NMR (CDCl₃, 400 MHz): δ 158.62 (Pr-C^{Pz}), 146.95 (Pz-C^{Pz}), 99.22 (H-C^{Pz}), 25.62 (Me₂CH), 23.35, 22.90 (CH₃)₂CH). Anal. Calc. (found) for C₁₂H₁₈N₄: C 66.02 (66.00), H 8.31 (8.22), N 25.67 (25.55).

Synthesis of D^{Ad}-H. This compound was obtained using a method similar to that for D^{Br}-H except 1-adamantyl methyl ketone was used in place of 4'-chloroacetophenone. Yield: 4.5 g (20%). ¹H NMR (DMSO-*d*₆, 400 MHz): δ 6.22 (s, 2H, Pz-H), 1.95, 1.81, 1.67 (br, 30H, Ad). ¹³C NMR (CDCl₃, 400 MHz): δ 164.10 (Ad-C^{Pz}),

142.44 (Pz-C^{Pz}), 102.35 (H-C^{Pz}), 42.66, 36.80, 33.51, 28.48 (Ad-C). Anal. Calcd (found) for C₂₆H₃₄N₄: C, 77.57 (77.2); H, 8.51 (8.49); N, 13.92 (13.69).

Synthesis of D^{Bu}₂Al₃Me₅. A mixture of D^{Bu}-H (0.45 g, 1.8 mmol) and AlMe₃ (11 mL, 2.0 M, 5.5 mmol) in THF (30 mL) was stirred overnight at room temperature. Volatile materials were removed under vacuum to give a white powder, and then hexane (40 mL) was transferred to give a suspension. A white powder was obtained after filtering. Yield: 0.49 g (85%). ¹H NMR (CDCl₃, 400 MHz): δ 6.69 (s, 2H, Pz-H), 1.52 (s, 18H, C(CH₃)₃), -0.18, -0.47 (s, 12H, Al^{terminal}(CH₃)₂), -0.99 (s, 3H, Al^{center}(CH₃)). ¹³C NMR (CDCl₃, 50 MHz): δ 168.23 (t-Bu-C^{Pz}), 144.71 (Pz-C^{Pz}), 100.62 (H-C^{Pz}), 32.97 (C(CH₃)₃), 31.76 (C(CH₃)₃), 0.10, -4.29 (Al(CH₃)₂), -9.23 (Al(CH₃)). Anal. Found (calcd) for D^{Bu}₂Al₃Me₅, C₃₃H₅₅Al₃N₈: C, 61.47 (61.52); N, 17.38 (17.56); H, 8.60 (8.81).

Synthesis of D^{Pr}₂Al₃Me₅. This compound was obtained using a method similar to that for D^{Bu}₂Al₃Me₅ except D^{Pr}-H was used in place of D^{Bu}-H. Yield: 0.32 g (80%). ¹H NMR (CDCl₃, 400 MHz): δ 6.37 (s, 4H, Pz-H), 3.35 (m, 4H, Me₂CH) 1.34 (m, 24H, (CH₃)₂CH), -0.42, -0.57 (s, 12H, Al^{terminal}(CH₃)₂), -0.94 (s, 3H, Al^{center}(CH₃)). ¹³C NMR (CDCl₃, 50 MHz): δ 164.97 (i-Pr-C^{Pz}), 145.22 (Pz-C^{Pz}), 97.84 (H-C^{Pz}), 27.26 (CH(CH₃)₂), 24.38, 23.18 (CH(CH₃)₂), -6.95, -8.23 (Al(CH₃)₂), -9.99 (Al(CH₃)). Anal. Found (calcd) for D^{Pr}₂Al₃Me₅, C₂₉H₄₇Al₃N₈: C, 59.17 (59.31); N, 19.03 (18.97); H, 8.05 (7.79).

Synthesis of D^{Ad}₂Al₃Me₅. This compound was obtained using a method similar to that for D^{Bu}₂Al₃Me₅ except D^{Ad}-H was used in place of D^{Bu}-H. Yield: 2.1 g (60%). ¹H NMR (CDCl₃, 400 MHz): δ 6.42 (s, 4H, Pz-H), 2.07, 1.74 (br, 60H, Ad), -0.28, -0.53 (s, 12H, Al^{terminal}(CH₃)₂), -1.22 (s, 3H, Al^{center}(CH₃)). ¹³C NMR (CDCl₃, 50 MHz): δ 168.88 (Ad-C^{Pz}), 145.00 (Pz-C^{Pz}), 100.21 (H-C^{Pz}), 42.74, 36.52, 35.44, 28.75 (Ad-C), -1.99, -3.38 (Al(CH₃)₂), -9.55 (Al(CH₃)). Anal. Found (calcd) for D^{Ad}₂Al₃Me₅, C₅₇H₇₉Al₃N₈: C, 71.52 (71.89); N, 11.71 (11.58); H, 8.32 (8.10).

Synthesis of D^{Ph}₂Al₃Me₅. This compound was obtained using a method similar to that for D^{Bu}₂Al₃Me₅ except D^{Ph}-H was used in place of D^{Bu}-H. Yield: 0.42 g (85%). ¹H NMR (CDCl₃, 400 MHz): δ 7.51–7.48, 7.41–7.39 (m, 20 H, Ar-H), 6.58 (s, 2H, Pz-H), -0.21, -0.42 (s, 12H, Al^{terminal}(CH₃)₂), -1.97 (s, 3H, Al^{center}(CH₃)). ¹³C NMR (CDCl₃, 50 MHz): δ 157.93 (Ph-C^{Pz}), 144.74 (Pz-C^{Pz}), 132.28, 129.19, 129.09, 128.52 (Ph), 101.91 (H-C^{Pz}), 0.08, -5.91 (Al(CH₃)₂), -9.83 (Al(CH₃)). Anal. Found (calcd) for D^{Ph}₂Al₃Me₅, C₄₁H₃₉Al₃N₈: C, 67.95 (67.88); N, 15.46 (15.51); H, 5.42 (5.33).

Synthesis of D^{tolyl}₂Al₃Me₅. This compound was obtained using a method similar to that for D^{Bu}₂Al₃Me₅ except D^{tolyl}-H was used in place of D^{Bu}-H. Yield: 0.47 g (75%). ¹H NMR (CDCl₃, 400 MHz): δ 7.30 (d, J = 8.0 Hz, 8H, m-CH₃-PhH), 7.12 (d, J = 8.0 Hz, 8H, o-CH₃-PhH), 6.45 (s, 4H, Pz-H), 2.29 (s, 12H, CH₃), -0.30, -2.00 (s, 12H, Al^{terminal}(CH₃)₂), -0.52 (s, 3H, Al^{center}(CH₃)). ¹³C NMR (CDCl₃, 50 MHz): δ 157.95 (Ph-C^{Pz}), 144.73 (Pz-C^{Pz}), 139.11, 129.46, 129.18, 128.98 (Ph), 101.75 (H-C^{Pz}), 21.42 (CH₃Ph) 1.12, -5.92 (Al(CH₃)₂), -9.49 (Al(CH₃)). Anal. Found (calcd) for D^{tolyl}₂Al₃Me₅, C₄₅H₄₇Al₃N₈: C, 69.22 (69.11); N, 14.35 (14.36); H, 6.07 (6.01).

General Procedures for the Polymerization of ε-Caprolactone. A typical polymerization procedure was exemplified by the synthesis in entry 1 of Table 2 using complex D^{Bu}₂Al₃Me₅ as a catalyst. The polymerization conversion was analyzed by ¹H NMR spectroscopic studies. Toluene (5.0 mL) was added to a mixture of the complex D^{Bu}₂Al₃Me₅ (0.25 mmol), BnOH (1.25 mmol), and ε-caprolactone (10 mmol) at room temperature. At indicated time intervals, 0.05 mL aliquots were removed, trapped with CDCl₃ (1 mL), and analyzed by ¹H NMR. After the solution was stirred for 150 min, the reaction mixture was then quenched by adding a drop of isopropyl alcohol, and the polymer precipitated as a white solid when it was poured into n-hexane (50.0 mL). The isolated white solid was dissolved in CH₂Cl₂ (5.0 mL), and water (10 mL) was used to wash the organic solution. Volatile materials were removed under vacuum to give a purified crystalline solid. Yield: 1.04 g (92%).

Computational Methods. The reaction mechanism was studied by DFT calculations at the B3LYP/6-31G(d) level.^{105,106} The calculations were carried out with Gaussian 09. The calculations of Gibbs free energy were done at 298.15 K under 1 atm. The minimum energy stationary point and the energy saddle point were confirmed by frequency analysis with the same calculation level.

■ ASSOCIATED CONTENT

Supporting Information

The Supporting Information is available free of charge at <https://pubs.acs.org/doi/10.1021/acs.inorgchem.1c01192>.

Polymer characterization data, details of the kinetic study (PDF)

Accession Codes

CCDC 1955471 contains the supplementary crystallographic data for this paper. These data can be obtained free of charge via www.ccdc.cam.ac.uk/data_request/cif, or by emailing data_request@ccdc.cam.ac.uk, or by contacting The Cambridge Crystallographic Data Centre, 12 Union Road, Cambridge CB2 1EZ, UK; fax: +44 1223 336033.

■ AUTHOR INFORMATION

Corresponding Authors

Kuo-Hui Wu – Department of Chemistry, National Central University, Taoyuan 32001, Taiwan, Republic of China; Email: wukuohui@ncu.edu.tw

Hsuan-Ying Chen – Department of Medicinal and Applied Chemistry, Drug Development and Value Creation Research Center, Kaohsiung Medical University, Kaohsiung 80708, Taiwan, Republic of China; Department of Chemistry, National Sun Yat-Sen University, Kaohsiung 80424, Taiwan, Republic of China; Department of Medical Research, Kaohsiung Medical University Hospital, Kaohsiung 80708, Taiwan, Republic of China; orcid.org/0000-0003-1424-3540; Phone: +886-7-3121101-2585; Email: hchen@kmu.edu.tw; Fax: +886-7-3125339

Authors

Someswara Rao Kosuru – Department of Medicinal and Applied Chemistry, Drug Development and Value Creation Research Center, Kaohsiung Medical University, Kaohsiung 80708, Taiwan, Republic of China

Feng-Jie Lai – Department of Dermatology, Chi Mei Medical Center, Tainan, Taiwan, Republic of China; Center for General Education, Southern Taiwan University of Science and Technology, Tainan, Taiwan, Republic of China

Yu-Lun Chang – Department of Medicinal and Applied Chemistry, Drug Development and Value Creation Research Center, Kaohsiung Medical University, Kaohsiung 80708, Taiwan, Republic of China

Chen-Yu Li – Department of Medicinal and Applied Chemistry, Drug Development and Value Creation Research Center, Kaohsiung Medical University, Kaohsiung 80708, Taiwan, Republic of China

Yi-Chun Lai – Department of Medicinal and Applied Chemistry, Drug Development and Value Creation Research Center, Kaohsiung Medical University, Kaohsiung 80708, Taiwan, Republic of China

Shangwu Ding – Department of Medicinal and Applied Chemistry, Drug Development and Value Creation Research Center, Kaohsiung Medical University, Kaohsiung 80708, Taiwan, Republic of China; Department of Chemistry,

National Sun Yat-Sen University, Kaohsiung 80424, Taiwan, Republic of China

Yung-Han Lo – Department of Chemistry, Faculty of Science and Technology, Keio University, Minato City 108-8345 Tokyo, Japan

Complete contact information is available at:

<https://pubs.acs.org/10.1021/acs.inorgchem.1c01192>

Author Contributions

○S.R.K. and F.-J.L. contributed equally.

Notes

The authors declare no competing financial interest.

ACKNOWLEDGMENTS

This study was supported by the Ministry of Science and Technology of Taiwan (Grant MOST 109-2113-M-037-006) and Kaohsiung Medical University “NSYSU-KMU JOINT RESEARCH PROJECT” (NSYSUKMU 107-P010 and KMU-DK109004). We thank the Center for Research Resources and Development at Kaohsiung Medical University for instrumentation and equipment support.

REFERENCES

- (1) Mato, Y.; Isobe, T.; Takada, H.; Ohtake, C.; Kaminuma, T. Plastic Resin Pellets as a Transport Medium for Toxic Chemicals in the Marine Environment. *Environ. Sci. Technol.* **2001**, *35*, 318–324.
- (2) Green, D. S.; Boots, B.; Blockley, D. J.; Rocha, C.; Thompson, R. Impacts of Discarded Plastic Bags on Marine Assemblages and Ecosystem Functioning. *Environ. Sci. Technol.* **2015**, *49*, 5380–9.
- (3) Jambeck, J. R.; Geyer, R.; Wilcox, C.; Siegler, T. R.; Perryman, M.; Andrady, A.; Narayan, R.; Law, K. L. Plastic Waste Inputs from Land into the Ocean. *Science* **2015**, *347*, 768–771.
- (4) Lamb, J. B.; Willis, B. L.; Fiorenza, E. A.; Couch, C. S.; Howard, R.; Rader, D. N.; True, J. D.; Kelly, L. A.; Ahmad, A.; Jompa, J.; Harvell, C. D. Plastic Waste Associated with Disease on Coral Reefs. *Science* **2018**, *359*, 460–462.
- (5) Woodruff, M. A.; Hutmacher, D. W. The Return of a Forgotten Polymer—Polycaprolactone in the 21st Century. *Prog. Polym. Sci.* **2010**, *35*, 1217–1256.
- (6) Kamaly, N.; Yameen, B.; Wu, J.; Farokhzad, O. C. Degradable Controlled-Release Polymers and Polymeric Nanoparticles: Mechanisms of Controlling Drug Release. *Chem. Rev.* **2016**, *116*, 2602–63.
- (7) Liu, K.; Jiang, X.; Hunziker, P. Carbohydrate-Based Amphiphilic Nano Delivery Systems for Cancer Therapy. *Nanoscale* **2016**, *8*, 16091–16156.
- (8) Palivan, C. G.; Goers, R.; Najer, A.; Zhang, X.; Car, A.; Meier, W. Bioinspired Polymer Vesicles and Membranes for Biological and medical applications. *Chem. Soc. Rev.* **2016**, *45*, 377–411.
- (9) Park, J. Y.; Gao, G.; Jang, J.; Cho, D.-W. 3D Printed Structures for Delivery of Biomolecules and Cells: Tissue Repair and Regeneration. *J. Mater. Chem. B* **2016**, *4*, 7521–7539.
- (10) Shukla, S. K.; Shukla, S. K.; Govender, P. P.; Giri, N. G. Biodegradable Polymeric Nanostructures in Therapeutic Applications: Opportunities and Challenges. *RSC Adv.* **2016**, *6*, 94325–94351.
- (11) Birnin-Yauri, A. U.; Ibrahim, N. A.; Zainuddin, N.; Abdan, K.; Then, Y. Y.; Chieng, B. W. Effect of Maleic Anhydride-Modified Poly(lactic acid) on the Properties of Its Hybrid Fiber Biocomposites. *Polymers* **2017**, *9*, 165–180.
- (12) Medel, S.; Syrova, Z.; Kovacic, L.; Hrdy, J.; Hornacek, M.; Jager, E.; Hruby, M.; Lund, R.; Cmarko, D.; Stepanek, P.; Raska, I.; Nyström, B. Curcumin-Bortezomib Loaded Polymeric Nanoparticles for Synergistic Cancer Therapy. *Eur. Polym. J.* **2017**, *93*, 116–131.
- (13) Watts, A.; Kurokawa, N.; Hillmyer, M. A. Strong, Resilient, and Sustainable Aliphatic Polyester Thermoplastic Elastomers. *Biomacromolecules* **2017**, *18*, 1845–1854.
- (14) Xiang, C.; Acevedo, N. C. In Situ Self-Assembled Nanocomposites from Bacterial Cellulose Reinforced with Electrospun Poly(lactic acid)/Lipids Nanofibers. *Polymers* **2017**, *9*, 179–191.
- (15) Bhowmick, S.; Thanusha, A. V.; Kumar, A.; Scharnweber, D.; Rother, S.; Koul, V. Nanofibrous Artificial Skin Substitute Composed of mPEG–PCL Grafted Gelatin/Hyaluronan/Chondroitin Sulfate/Serinin for 2nd Degree Burn Care: in Vitro and in Vivo Study. *RSC Adv.* **2018**, *8*, 16420–16432.
- (16) Slater, B.; Wong, S. O.; Duckworth, A.; White, A. J. P.; Hill, M. R.; Ladewig, B. P. Upcycling a Plastic Cup: One-Pot Synthesis of Lactate Containing Metal Organic Frameworks from Poly(lactic acid). *Chem. Commun.* **2019**, *55*, 7319–7322.
- (17) Ramot, Y.; Haim-Zada, M.; Domb, A. J.; Nyska, A. Biocompatibility and Safety of PLA and Its Copolymers. *Adv. Drug Delivery Rev.* **2016**, *107*, 153–162.
- (18) Carosio, F.; Colonna, S.; Fina, A.; Rydzek, G.; Hemmerlé, J.; Jierry, L.; Schaaf, P.; Boulmedais, F. Efficient Gas and Water Vapor Barrier Properties of Thin Poly(lactic acid) Packaging Films: Functionalization with Moisture Resistant Nafion and Clay Multilayers. *Chem. Mater.* **2014**, *26*, 5459–5466.
- (19) Huang, B. H.; Tsai, C. Y.; Chen, C. T.; Ko, B. T. Metal Complexes Containing Nitrogen-Heterocycle Based Aryloxide or Arylamido Derivatives as Discrete Catalysts for Ring-Opening Polymerization of Cyclic Esters. *Dalton Trans.* **2016**, *45*, 17557–17580.
- (20) Redshaw, C. Metallocalixarene Catalysts: Alpha-Olefin Polymerization and ROP of Cyclic Esters. *Dalton Trans.* **2016**, *45*, 9018–30.
- (21) Wei, Y.; Wang, S.; Zhou, S. Aluminum Alkyl Complexes: Synthesis, Structure, and Application in ROP of Cyclic Esters. *Dalton Trans.* **2016**, *45*, 4471–85.
- (22) Chang, Y. A.; Waymouth, R. M. Recent Progress on the Synthesis of Cyclic Polymers via Ring-Expansion Strategies. *J. Polym. Sci., Part A: Polym. Chem.* **2017**, *55*, 2892–2902.
- (23) Fuoco, T.; Pappalardo, D. Aluminum Alkyl Complexes Bearing Salicylaldehyde Ligands: Versatile Initiators in the Ring-Opening Polymerization of Cyclic Esters. *Catalysts* **2017**, *7*, 64.
- (24) Osten, K. M.; Mehrhodavandi, P. Indium Catalysts for Ring Opening Polymerization: Exploring the Importance of Catalyst Aggregation. *Acc. Chem. Res.* **2017**, *50*, 2861–2869.
- (25) Redshaw, C. Use of Metal Catalysts Bearing Schiff Base Macrocycles for the Ring Opening Polymerization (ROP) of Cyclic Esters. *Catalysts* **2017**, *7*, 165–175.
- (26) Ligny, R.; Hanninen, M. M.; Guillaume, S. M.; Carpentier, J. F. Steric vs. Electronic Stereocontrol in Syndio- or Iso-Selective ROP of Functional Chiral Beta-Lactones Mediated by Achiral Yttrium-Bisphenolate Complexes. *Chem. Commun.* **2018**, *54*, 8024–8031.
- (27) Stirling, E.; Champouret, Y.; Visseaux, M. Catalytic Metal-Based Systems for Controlled Statistical Copolymerisation of Lactide with a Lactone. *Polym. Chem.* **2018**, *9*, 2517–2531.
- (28) Kremer, A. B.; Mehrhodavandi, P. Dinuclear Catalysts for the Ring Opening Polymerization of Lactide. *Coord. Chem. Rev.* **2019**, *380*, 35–57.
- (29) Kosuru, S. R.; Sun, T. H.; Wang, L. F.; Vandavasi, J. K.; Lu, W. Y.; Lai, Y. C.; Hsu, S. C. N.; Chiang, M. Y.; Chen, H. Y. Enhanced Catalytic Activity of Aluminum Complexes for the Ring-Opening Polymerization of Epsilon-Caprolactone. *Inorg. Chem.* **2017**, *56*, 7998–8006.
- (30) Wang, P.; Chao, J.; Chen, X. Living Ring-Opening Polymerization of Epsilon-Caprolactone Catalyzed by Beta-Quinolyl-Enamino Aluminium Complexes: Ligand Electronic Effects. *Dalton Trans.* **2018**, *47*, 4118–4127.
- (31) Chang, C.-C.; Chang, Y.-C.; Lu, W.-Y.; Lai, Y.-C.; Wu, K.-H.; Lin, Y.-F.; Chen, H.-Y. Novel Aluminum Complexes Bearing 2-(Aminomethylene)malonate Ligands with High Efficiency and Controllability in Ring-Opening Polymerization of ϵ -Caprolactone. *Eur. Polym. J.* **2019**, *115*, 399–408.
- (32) Qin, L.; Zhang, Y.; Chao, J.; Cheng, J.; Chen, X. Four- and Five-Coordinate Aluminum Complexes Supported by N,O-Bidentate

Beta-Pyrazulenolate Ligands: Synthesis, Structure and Application in ROP of Epsilon-Caprolactone and Lactide. *Dalton Trans.* **2019**, *48*, 12315–12325.

(33) Huang, T. W.; Su, R. R.; Lin, Y. C.; Lai, H. Y.; Yang, C. Y.; Senadi, G. C.; Lai, Y. C.; Chiang, M. Y.; Chen, H. Y. Improvement in Aluminum Complexes Bearing a Schiff Base in Ring-Opening Polymerization of Epsilon-Caprolactone: the Synergy of the N,S-Schiff Base in a Five-Membered Ring Aluminum System. *Dalton Trans.* **2018**, *47*, 15565–15573.

(34) Macaranas, J. A.; Luke, A. M.; Mandal, M.; Neisen, B. D.; Marell, D. J.; Cramer, C. J.; Tolman, W. B. Sterically Induced Ligand Framework Distortion Effects on Catalytic Cyclic Ester Polymerizations. *Inorg. Chem.* **2018**, *57*, 3451–3457.

(35) Chumsaeng, P.; Haesuwannakij, S.; Virachotikul, A.; Phomphrai, K. Random Copolymerization of L-Lactide and ϵ -Caprolactone by Aluminum Alkoxide Complexes Supported by N₂O₂ Bis(phenolate)-Amine Ligands. *J. Polym. Sci., Part A: Polym. Chem.* **2019**, *57*, 1635–1644.

(36) Li, M.; Behzadi, S.; Chen, M.; Pang, W.; Wang, F.; Tan, C. Phenoxyimine Ligands Bearing Nitrogen-Containing Second Coordination Spheres for Zinc Catalyzed Stereoselective Ring-Opening Polymerization of rac-Lactide. *Organometallics* **2019**, *38*, 461–468.

(37) Plommer, H.; Murphy, J. N.; Dawe, L. N.; Kerton, F. M. Morpholine-Stabilized Cationic Aluminum Complexes and Their Reactivity in Ring-Opening Polymerization of epsilon-Caprolactone. *Inorg. Chem.* **2019**, *58*, S253–S264.

(38) Chen, L.; Li, W.; Yuan, D.; Zhang, Y.; Shen, Q.; Yao, Y. Syntheses of Mononuclear and Dinuclear Aluminum Complexes Stabilized by Phenolato Ligands and Their Applications in the Polymerization of epsilon-Caprolactone: A Comparative Study. *Inorg. Chem.* **2015**, *54*, 4699–708.

(39) Huang, H.-C.; Wang, B.; Zhang, Y.-P.; Li, Y.-S. Bimetallic Aluminum Complexes with Cyclic β -Ketiminato Ligands: the Cooperative Effect Improves Their Capability in Polymerization of Lactide and ϵ -Caprolactone. *Polym. Chem.* **2016**, *7*, 5819–5827.

(40) Beament, J.; Mahon, M. F.; Buchard, A.; Jones, M. D. Aluminum Complexes of Monopyrrolidine Ligands for the Controlled Ring-Opening Polymerization of Lactide. *Organometallics* **2018**, *37*, 1719–1724.

(41) Duda, A.; Florjanczyk, Z.; Hofman, A.; Slomkowski, S.; Penczek, S. Living Pseudoanionic Polymerization of ϵ -Caprolactone. Poly(ϵ -caprolactone) Free of Cyclics and with Controlled End Groups. *Macromolecules* **1990**, *23*, 1640–1646.

(42) Yu, Y.; Fischer, E. J.; Storti, G.; Morbidelli, M. Modeling of Molecular Weight Distribution in Ring-Opening Polymerization of L,L-Lactide. *Ind. Eng. Chem. Res.* **2014**, *53*, 7333–7342.

(43) Lian, B.; Thomas, C. M.; Casagrande, O. L.; Lehmann, C. W.; Roisnel, T.; Carpentier, J. F. Aluminum and Zinc Complexes Based on an Amino-Bis(pyrazolyl) Ligand: Synthesis, Structures, and Use in MMA and Lactide Polymerization. *Inorg. Chem.* **2007**, *46*, 328–340.

(44) Milione, S.; Grisi, F.; Centore, R.; Tuzi, A. Neutral and Cationic Heteroscorpionate Aluminum Complexes: Synthesis, Structure, and Ring-Opening Polymerization of ϵ -Caprolactone. *Organometallics* **2006**, *25*, 266–274.

(45) Chai, Z.-Y.; Zhang, C.; Wang, Z.-X. Synthesis, Characterization, and Catalysis in ϵ -Caprolactone Polymerization of Aluminum and Zinc Complexes Supported by N,N,N-Chelate Ligands. *Organometallics* **2008**, *27*, 1626–1633.

(46) Silvestri, A.; Grisi, F.; Milione, S. Ring Opening Polymerization of Lactide Promoted by Alcoholized Heteroscorpionate Aluminum Complexes. *J. Polym. Sci., Part A: Polym. Chem.* **2010**, *48*, 3632–3639.

(47) Otero, A.; Lara-Sánchez, A. n.; Fernández-Baeza, J.; Alonso-Moreno, C.; Castro-Osma, J. A.; Márquez-Segovia, I.; Sánchez-Barba, L. F.; Rodríguez, A. M.; García-Martínez, J. C. Neutral and Cationic Aluminum Complexes Supported by Acetamidate and Thioacetamidate Heteroscorpionate Ligands as Initiators for Ring-Opening Polymerization of Cyclic Esters. *Organometallics* **2011**, *30*, 1507–1522.

(48) Huang, T.-L.; Chen, C.-T. Aluminium Complexes Containing Pyrazolyl–Phenolate Ligands as Catalysts for Ring Opening Polymerization of ϵ -Caprolactone. *J. Organomet. Chem.* **2013**, *725*, 15–21.

(49) Rufino-Felipe, E.; Lopez, N.; Vengoechea-Gómez, F. A.; Guerrero-Ramírez, L.-G.; Muñoz-Hernández, M.-Á. Ring-Opening Polymerization of rac-Lactide Catalyzed by Al(III) and Zn(II) Complexes Incorporating Schiff Base Ligands Derived from Pyrrole-2-Carboxaldehyde. *Appl. Organomet. Chem.* **2018**, *32*, e4315–e4324.

(50) Shironina, T. M.; Igidov, N. M.; Koz'minykh, E. N.; Kon'shina, L. O.; Kasatkina, Y. S.; Koz'minykh, V. O. 1,3,4,6-Tetracarboxyl Compounds: IV.* Reaction of 3,4-Dihydroxy-2,4-hexadiene-1,6-diones with Hydrazine and Arylhydrazines. *Russ. J. Org. Chem.* **2001**, *37*, 1486–1494.

(51) Storch, G.; Spallek, M. J.; Rominger, F.; Trapp, O. Tautomerization-Mediated Molecular Switching between Six- and Seven-Membered Rings Stabilized by Hydrogen Bonding. *Chem. - Eur. J.* **2015**, *21*, 8939–45.

(52) Aida, T.; Inoue, S. Metalloporphyrins as Initiators for Living and Immortal Polymerizations. *Acc. Chem. Res.* **1996**, *29*, 39–48.

(53) Ajellal, N.; Lyubov, D. M.; Sinenkov, M. A.; Fukin, G. K.; Cherkasov, A. V.; Thomas, C. M.; Carpentier, J. F.; Trifonov, A. A. Bis(guanidinate) Alkoxide Complexes of Lanthanides: Synthesis, Structures and Use in Immortal and Stereoselective Ring-Opening Polymerization of Cyclic Esters. *Chem. - Eur. J.* **2008**, *14*, 5440–8.

(54) Rosen, T.; Goldberg, I.; Navarra, W.; Venditto, V.; Kol, M. Divergent [ONNN]Mg-Cl Complexes in Highly Active and Living Lactide Polymerization. *Chem. Sci.* **2017**, *8*, 5476–5481.

(55) Wang, B.; Zhao, H.; Wang, L.; Sun, J.; Zhang, Y.; Cao, Z. Immortal Ring-Opening Polymerization of Lactides with Super High Monomer to Catalyst Ratios Initiated by Zirconium and Titanium Complexes Containing Multidentate Amino-Bis(phenolate) Ligands. *New J. Chem.* **2017**, *41*, S669–S677.

(56) Wilson, J. A.; Hopkins, S. A.; Wright, P. M.; Dove, A. P. 'Immortal' Ring-Opening Polymerization of ω -Pentadecalactone by Mg(BHT)₂(THF)₂. *Polym. Chem.* **2014**, *5*, 2691–2694.

(57) Ma, H.; Okuda, J. Kinetics and Mechanism of L-Lactide Polymerization by Rare Earth Metal Silylamido Complexes: Effect of Alcohol Addition. *Macromolecules* **2005**, *38*, 2665–2673.

(58) Bridier, B.; Lopez, N.; Perez-Ramirez, J. Molecular Understanding of Alkyne Hydrogenation for the Design of Selective Catalysts. *Dalton Trans* **2010**, *39*, 8412–8419.

(59) Amgoune, A.; Thomas, C. M.; Roisnel, T.; Carpentier, J. F. Ring-Opening Polymerization of Lactide with Group 3 Metal Complexes Supported by Dianionic Alkoxy-Amino-Bisphenolate Ligands: Combining High Activity, Productivity, and Selectivity. *Chem. - Eur. J.* **2006**, *12*, 169–179.

(60) Nuyken, O.; Pask, S. Ring-Opening Polymerization—An Introductory Review. *Polymers* **2013**, *5*, 361–403.

(61) Hsu, C.-Y.; Tseng, H.-C.; Vandavasi, J. K.; Lu, W.-Y.; Wang, L.-F.; Chiang, M. Y.; Lai, Y.-C.; Chen, H.-Y.; Chen, H.-Y. Investigation of the Dinuclear Effect of Aluminum Complexes in the Ring-Opening Polymerization of ϵ -Caprolactone. *RSC Adv.* **2017**, *7*, 18851–18860.

(62) Pykko, P.; Atsumi, M. Molecular Single-Bond Covalent Radii for Elements 1–118. *Chem. - Eur. J.* **2009**, *15*, 186–97.

(63) Batsanov, S. S. Van der Waals Radii of Elements. *Inorg. Mater.* **2001**, *37*, 871–885.

(64) Nishio, M. The CH/ π Hydrogen bond in chemistry. Conformation, Supramolecules, Optical Resolution and Interactions Involving Carbohydrates. *Phys. Chem. Chem. Phys.* **2011**, *13*, 13873–13900.

(65) Marlier, E. E.; Macaranas, J. A.; Marell, D. J.; Dunbar, C. R.; Johnson, M. A.; DePorre, Y.; Miranda, M. O.; Neisen, B. D.; Cramer, C. J.; Hillmyer, M. A.; Tolman, W. B. Mechanistic Studies of epsilon-Caprolactone Polymerization by (salen)AlOR Complexes and a Predictive Model for Cyclic Ester Polymerizations. *ACS Catal.* **2016**, *6*, 1215–1224.

(66) Li, Y.; Zhao, K.-Q.; Elsegood, M. R. J.; Prior, T. J.; Sun, X.; Mo, S.; Redshaw, C. Organoaluminum Complexes of ortho-, meta-, para-

Anisidines: Synthesis, Structural Studies and ROP of ϵ -Caprolactone (and rac-Lactide). *Catal. Sci. Technol.* **2014**, *4*, 3025–3031.

(67) Hsu, C.-Y.; Tseng, H.-C.; Vandavasi, J. K.; Lu, W.-Y.; Wang, L.-F.; Chiang, M. Y.; Lai, Y.-C.; Chen, H.-Y.; Chen, H.-Y. Investigation of the Dinuclear Effect of Aluminum Complexes in the Ring-Opening Polymerization of ϵ -Caprolactone. *RSC Adv.* **2017**, *7*, 18851–18860.

(68) Chang, M. C.; Lu, W. Y.; Chang, H. Y.; Lai, Y. C.; Chiang, M. Y.; Chen, H. Y.; Chen, H. Y. Comparative Study of Aluminum Complexes Bearing N,O- and N,S-Schiff Base in Ring-Opening Polymerization of epsilon-Caprolactone and L-Lactide. *Inorg. Chem.* **2015**, *54*, 11292–11298.

(69) Lee, C.-L.; Lin, Y.-F.; Jiang, M.-T.; Lu, W.-Y.; Vandavasi, J. K.; Wang, L.-F.; Lai, Y.-C.; Chiang, M. Y.; Chen, H.-Y. Improvement in Aluminum Complexes Bearing Schiff Bases in Ring-Opening Polymerization of ϵ -Caprolactone: A Five-Membered-Ring System. *Organometallics* **2017**, *36*, 1936–1945.

(70) Huang, T. W.; Su, R. R.; Lin, Y. C.; Lai, H. Y.; Yang, C. Y.; Senadi, G. C.; Lai, Y. C.; Chiang, M. Y.; Chen, H. Y. Improvement in Aluminum Complexes Bearing a Schiff Base in Ring-Opening Polymerization of epsilon-Caprolactone: the Synergy of the N,S-Schiff Base in a Five-Membered Ring Aluminum System. *Dalton Trans.* **2018**, *47*, 15565–15573.

(71) Lu, W.-Y.; Chang, Y.-C.; Lian, C.-J.; Wu, K.-H.; Chiang, M. Y.; Chen, H.-Y.; Lin, C.-C.; Ko, B.-T. Optimization of Six-Membered ring Aluminum Complexes in ϵ -Caprolactone Polymerization. *Eur. Polym. J.* **2019**, *114*, 151–163.

(72) Huang, T.-L.; Chen, C.-T. Aluminium Complexes Containing Pyrazolyl-Phenolate Ligands as Catalysts for Ring Opening Polymerization of ϵ -Caprolactone. *J. Organomet. Chem.* **2013**, *725*, 15–21.

(73) Tseng, H. C.; Chiang, M. Y.; Lu, W. Y.; Chen, Y. J.; Lian, C. J.; Chen, Y. H.; Tsai, H. Y.; Lai, Y. C.; Chen, H. Y. A Closer Look at epsilon-Caprolactone Polymerization Catalyzed by Alkyl Aluminum Complexes: The Effect of Induction Period on Overall Catalytic Activity. *Dalton Trans.* **2015**, *44*, 11763–73.

(74) Alcazar-Roman, L. M.; O'Keefe, B. J.; Hillmyer, M. A.; Tolman, W. B. Electronic Influence of Ligand Substituents on the Rate of Polymerization of ϵ -Caprolactone by Single-Site Aluminium Alkoxide Catalysts. *Dalton Trans.* **2003**, 3082–3087.

(75) Ikpo, N.; Barbon, S. M.; Drover, M. W.; Dawe, L. N.; Kerton, F. M. Aluminum Methyl and Chloro Complexes Bearing Monoanionic Aminophenolate Ligands: Synthesis, Characterization, and Use in Polymerizations. *Organometallics* **2012**, *31*, 8145–8158.

(76) Wei, J.; Riffel, M. N.; Diaconescu, P. L. Redox Control of Aluminum Ring-Opening Polymerization: A Combined Experimental and DFT Investigation. *Macromolecules* **2017**, *50*, 1847–1861.

(77) Alkarekshi, W.; Armitage, A. P.; Boyron, O.; Davies, C. J.; Govere, M.; Gregory, A.; Singh, K.; Solan, G. A. Phenolate Substituent Effects on Ring-Opening Polymerization of ϵ -Caprolactone by Aluminum Complexes Bearing 2-(Phenyl-2-olate)-6-(1-amidoalkyl)pyridine Pincers. *Organometallics* **2013**, *32*, 249–259.

(78) Gesslbauer, S.; Hutchinson, G.; White, A. J. P.; Burés, J.; Romain, C. Chirality-Induced Catalyst Aggregation: Insights into Catalyst Speciation and Activity Using Chiral Aluminum Catalysts in Cyclic Ester Ring-Opening Polymerization. *ACS Catal.* **2021**, *11*, 4084–4093.

(79) Hsieh, Y.-L.; Huang, N.; Lee, G.-H.; Peng, C.-H. Bipyridine-Phenolate Based Aluminum Complexes Mediated Ring-Opening Polymerization of ϵ -Caprolactone and Lactides with a High Stereoselectivity. *Polymer* **2015**, *72*, 281–291.

(80) Wang, P.; Hao, X.; Cheng, J.; Chao, J.; Chen, X. Aluminum Chelates Supported by beta-Quinolyl Enolate Ligands: Synthesis and ROP of epsilon-CL. *Dalton Trans.* **2016**, *45*, 9088–96.

(81) Chen, C.-T.; Liao, C.-H.; Peng, K.-F.; Chen, M.-T.; Huang, T.-L. Synthesis, Characterization and Catalytic Studies of Aluminium Complexes Containing Sulfonylamido-Oxazolinolate or -Pyrazolinolate Ligands. *J. Organomet. Chem.* **2014**, *753*, 9–19.

(82) Castro-Osma, J. A.; Alonso-Moreno, C.; Lara-Sanchez, A.; Otero, A.; Fernandez-Baeza, J.; Sanchez-Barba, L. F.; Rodriguez, A. M. Catalytic Behaviour in the Ring-Opening Polymerisation of Organo-

aluminiums Supported by Bulky Heteroscorpionate Ligands. *Dalton Trans.* **2015**, *44*, 12388–12400.

(83) Bouyahyi, M.; Grunova, E.; Marquet, N.; Kirillov, E.; Thomas, C. M.; Roisnel, T.; Carpentier, J. F. Aluminum Complexes of Fluorinated Dialkoxy-Diimino Salen-like Ligand: Synthesis, Structures, and Use in Ring-Opening Polymerization of Cyclic Esters. *Organometallics* **2008**, *27*, 5815–5825.

(84) Amgoune, A.; Lavanant, L.; Thomas, C. M.; Chi, Y.; Welter, R.; Dagorne, S.; Carpentier, J. F. Chelation Effect in Polymerization of Cyclic Esters by Metal Alkoxides: Structure Characterization of the Intermediate Formed by Primary Insertion of Lactide into the Al-OR Bond of an Organometallic Initiator. *Organometallics* **2005**, *24*, 6279–6282.

(85) Kazarina, O. V.; Gourlaouen, C.; Karmazin, L.; Morozov, A. G.; Fedushkin, I. L.; Dagorne, S. Low Valent Al(ii)-Al(ii) Catalysts as Highly Active epsilon-Caprolactone Polymerization Catalysts: Indication of Metal Cooperativity through DFT Studies. *Dalton Trans.* **2018**, *47*, 13800–13808.

(86) Wu, C.; Zhou, H.; He, M.; Su, Q.; Li, G.; Wu, Q.; Mu, Y. Binuclear Aluminum Complexes with Amine-Imine Type Ligands Derived from 1,3-Benzenedialdehyde: Synthesis, Structures and Their Catalytic Properties in Ring-Opening Polymerization. *J. Coord. Chem.* **2016**, *69*, 1066–1075.

(87) Wei, C.; Han, B.; Zheng, D.; Zheng, Q.; Liu, S.; Li, Z. Aluminum Complexes Bearing Bidentate Amido-Phosphine Ligands for Ring-Opening Polymerization of ϵ -Caprolactone: Steric Effect on Coordination Chemistry and Reactivity. *Organometallics* **2019**, *38*, 3816–3823.

(88) Li, G.; Lamberti, M.; Pappalardo, D.; Pellicchia, C. Random Copolymerization of ϵ -Caprolactone and Lactides Promoted by Pyrrolylpyridylamido Aluminum Complexes. *Macromolecules* **2012**, *45*, 8614–8620.

(89) Hsiao, H.-C.; Datta, A.; Chen, Y.-F.; Chang, W.; Lee, T.-Y.; Lin, C.-H.; Huang, J.-H. Structural Aspects and Ring Opening Polymerization of ϵ -Caprolactone Using Mono- and Di-aluminum Compounds Incorporating Bidentate Pyrrole-Morpholine Ligands. *J. Organomet. Chem.* **2016**, *804*, 35–41.

(90) Armitage, A.; Boyron, O.; Champouret, Y.; Patel, M.; Singh, K.; Solan, G. Dimethyl-Aluminium Complexes Bearing Naphthyl-Substituted Pyridine-Alkylamides as Pro-Initiators for the Efficient ROP of ϵ -Caprolactone. *Catalysts* **2015**, *5*, 1425–1444.

(91) Huang, C.-H.; Wang, F.-C.; Ko, B. T.; Yu, T.-L.; Lin, C. C. Ring-Opening Polymerization of ϵ -Caprolactone and L-Lactide Using Aluminum Thiolates as Initiator. *Macromolecules* **2001**, *34*, 356–361.

(92) Tseng, H.-C.; Chen, F.-S.; Chiang, M. Y.; Lu, W.-Y.; Chen, Y.-H.; Lai, Y.-C.; Chen, H.-Y. Optimizing Ring-Opening Polymerization of ϵ -Caprolactone by Using Aluminum Complexes Bearing Amide as Catalysts and Their Application in Synthesizing Poly- ϵ -Caprolactone with Special Initiators and Other Polycycloesters. *RSC Adv.* **2015**, *5*, 90682–90690.

(93) Zhang, W.; Wang, Y.; Cao, J.; Wang, L.; Pan, Y.; Redshaw, C.; Sun, W.-H. Synthesis and Characterization of Dialkylaluminum Amidates and Their Ring-Opening Polymerization of ϵ -Caprolactone. *Organometallics* **2011**, *30*, 6253–6261.

(94) Koller, J. r.; Bergman, R. G. Highly Efficient Aluminum-Catalyzed Ring-Opening Polymerization of Cyclic Carbonates, Lactones, and Lactides, Including a Unique Crystallographic Snapshot of an Intermediate. *Organometallics* **2011**, *30*, 3217–3224.

(95) Wang, X.; Zhao, K.-Q.; Al-Khafaji, Y.; Mo, S.; Prior, T. J.; Elsegood, M. R. J.; Redshaw, C. Organoaluminium Complexes Derived from Anilines or Schiff Bases for the Ring-Opening Polymerization of ϵ -Caprolactone, δ -Valerolactone and rac-Lactide. *Eur. J. Inorg. Chem.* **2017**, *2017*, 1951–1965.

(96) Chakraborty, D.; Chen, E. Y.-X. Neutral, Three-Coordinate, Chelating Diamide Aluminum Complexes: Catalysts/Initiators for Synthesis of Telechelic Oligomers and High Polymers. *Organometallics* **2002**, *21*, 1438–1442.

(97) D'Auria, I.; Lamberti, M.; Mazzeo, M.; Milione, S.; Pellicchia, C. Phosphido-diphosphine pincer aluminum complexes as catalysts

for ring opening polymerization of cyclic esters. *J. Polym. Sci., Part A: Polym. Chem.* **2014**, *52*, 49–60.

(98) Hild, F.; Neehaul, N.; Bier, F.; Wirsum, M.; Gourlaouen, C.; Dagorne, S. Synthesis and Structural Characterization of Various N,O,N'-Chelated Aluminum and Gallium Complexes for the Efficient ROP of Cyclic Esters and Carbonates: How Do Aluminum and Gallium Derivatives Compare? *Organometallics* **2013**, *32*, 587–598.

(99) Ziemkowska, W.; Kucharski, S.; Kołodziej, A.; Anulewicz-Ostrowska, R. Reactions of Alkylalane Diolates with Water Synthesis, Characterisation and ϵ -Caprolactone Polymerisation Activity of Novel Alane Benzopinacolates. *J. Organomet. Chem.* **2004**, *689*, 2930–2939.

(100) Huang, Y.-T.; Wang, W.-C.; Hsu, C.-P.; Lu, W.-Y.; Chuang, W.-J.; Chiang, M. Y.; Lai, Y.-C.; Chen, H.-Y. The Ring-Opening Polymerization of ϵ -Caprolactone and L-Lactide Using Aluminum Complexes Bearing Benzothiazole Ligands as Catalysts. *Polym. Chem.* **2016**, *7*, 4367–4377.

(101) Chang, C.-J.; Chiu, C.-F.; Wu, K.-H.; Chang, Y.-L.; Lai, Y.-C.; Ding, S.; Chen, H.-Y. N-heterocyclic ligand optimization for aluminum complexes in ϵ -caprolactone and L-Lactide polymerization. *Polymer* **2020**, *202*, 122572.

(102) Ziemkowska, W.; Kochanowski, J.; Cyrański, M. K. Synthesis, structures and ϵ -caprolactone polymerization activity of aluminum N,N'-dimethyloxalamidates. *J. Organomet. Chem.* **2010**, *695*, 1205–1209.

(103) Wang, Q.; Zhao, W.; He, J.; Zhang, Y.; Chen, E. Y. X. Living Ring-Opening Polymerization of Lactones by N-Heterocyclic Olefin/ $\text{Al}(\text{C}_6\text{F}_5)_3$ Lewis Pairs: Structures of Intermediates, Kinetics, and Mechanism. *Macromolecules* **2017**, *50*, 123–136.

(104) Jozak, T.; Zabel, D.; Schubert, A.; Sun, Y.; Thiel, W. R. Ruthenium Complexes Bearing N-H Acidic Pyrazole Ligands. *Eur. J. Inorg. Chem.* **2010**, *2010*, 5135–5145.

(105) Becke, A. D. Density-Functional Thermochemistry. III. The Role of Exact Exchange. *J. Chem. Phys.* **1993**, *98*, 5648–5652.

(106) Lee, C.; Yang, W.; Parr, R. G. Development of the Colle-Salvetti Correlation-Energy Formula into a Functional of the Electron Density. *Phys. Rev. B: Condens. Matter Mater. Phys.* **1988**, *37*, 785–789.